353244

1. Report No. ATC-170	2. Government Accession No. DOT/FAA/TS-89/9	3. Recipient's Catalog No.
4. Title and Subtitle Microburst Observability and Frequency During 1988 in Denver, CO		5. Report Date 14 May 1990
		6. Performing Organization Code
7. Author(s) John T. DiStefano and David A. Clark		8. Performing Organization Report No. ATC-170
9. Performing Organization Name and Address Lincoln Laboratory, MIT P.O. Box 73 Lexington, MA 02173-9108		10. Work Unit No. (TRAIS)
		11. Contract or Grant No. DTFA-01-L-83-4-10579
12. Sponsoring Agency Name and Address Department of Transportation Federal Aviation Administration Systems Research and Development Service Washington, DC 20591		13. Type of Report and Period Covered Project Report
		14. Sponsoring Agency Code

15. Supplementary Notes

16. Abstract

    The observability of microbursts with single-Doppler radar is investigated through comparison of radar data and surface weather sensor data. The data were collected during 1988 in Denver, CO as part of the FAA Terminal Doppler Weather Radar measurement program. Radar data were collected by both an S-band and C-band radar, while surface data were taken from a mesoscale network of 42 weather sensors in the vicinity of Denver's Stapleton International Airport. Results are compared with previous similar studies of observability using data from 1987 in Denver, and 1986 in Huntsville, AL.

    A total of 184 microbursts impacting the surface mesonet were identified. For those microbursts for which both radar and surface data were available, 97% were observable by single-Doppler radar. This compares to 94% observability during 1987 in Denver, and 98% during 1986 in Huntsville. Two strong microbursts (at least 20 m/s differential velocity) were unobservable by radar throughout their lifetime: one due to low signal-to-noise ratio, and the other due initially to an asymmetric outflow with low signal-to-noise ratio also a contributing factor. Two other microbursts, with differential velocities from 10-19 m/s, were unobservable by radar: one due to shallow outflow with a depth limited to a height below that of the radar beam, and one due to asymmetric outflow oriented unfavorably with respect to the radar viewing angle.

    Consistent with previous observations, microburst occurrence was most frequent during June and July, when 94 microbursts were identified on 20 days. An anomalously high frequency was also seen in April, although the strength of these events was relatively modest. As expected, the diurnal distribution shows the late afternoon to be the most favorable time for microburst development; more than half of all events reached their maximum strength between the hours of 2-5 p.m. local time.

17. Key Words		18. Distribution Statement
Terminal Doppler Weather Radar wind divergence observability differential velocity	mesonet microburst wind shear	Document is available to the public through the National Technical Information Service, Springfield, VA 22161.

19. Security Classif. (of this report) Unclassified	20. Security Classif. (of this page) Unclassified	21. No. of Pages 58	22. Price

ACKNOWLEDGMENTS

TABLE OF CONTENTS

LIST OF ILLUSTRATIONS

LIST OF TABLES

ACRONYMS

AGL	Above Ground Level
FAA	Federal Aviation Administration
FL-2	FAA/Lincoln Laboratory Test-bed Doppler Radar
FLOWS	FAA/Lincoln Laboratory Observational Weather Studies
LLWAS	Low-Level Windshear Alert System
Max ΔV	Maximum Differential Velocity
Mesonet	Mesoscale network of surface weather sensors
SCR	Signal-to-Clutter Ratio
SNR	Signal-to-Noise Ratio
TDWR	Terminal Doppler Weather Radar
UND	University of North Dakota
UTC	Universal Time Coordinated (same as Greenwich Mean Time)

I. INTRODUCTION

The Federal Aviation Administration is currently procuring deployment of a network of Terminal Doppler Weather Radars (TDWRs) to automate detection and warning of hazardous weather in the vicinity of major U.S. airports. Of primary significance is the detection of wind shear associated with small-scale (less than 4 km horizontal extent) and potentially violent downdrafts of air known as microbursts. Microbursts have been shown to be a serious threat to aviation safety, particularly in the terminal area upon take-off and landing (Fujita, 1980; National Research Council, 1983; Fujita, 1985). TDWR applies pattern recognition algorithms to continually updated radar reflectivity and radial velocity data in order to detect and alert of developing microburst wind shear (Campbell and Merritt, 1987).

Successful performance of the TDWR system in an operational environment requires a high probability of wind shear detection while maintaining a low rate of false alarms. System performance is dually dependent upon the radar's sensing capabilities and limitations, and the performance of the microburst detection algorithm in properly recognizing patterns in the radar data, particularly in the Doppler velocity field (Campbell et al., 1989). The distinction between these two factors is illustrated in Fig. I-1. The "observability" of microbursts by Doppler radar can be viewed as the ability of the radar to show a signature in the Doppler field when a microburst is present, whereas "detectability" in this context is the algorithm's ability to properly interpret the Doppler field and recognize the signature. As such, evaluation of overall system performance is dependent upon both of these factors. Considerable attention has been devoted to assessing the latter, i.e. performance of the pattern recognition algorithm. This is typically done by comparing algorithm alerts to the divergence areas identified via manual analysis of radar data, either single- or dual-Doppler, by experienced radar meteorologists. The objective here, however, is to use both surface and radar data to estimate the frequency with which microbursts are "unobservable", showing no recognizable pattern in the Doppler field.
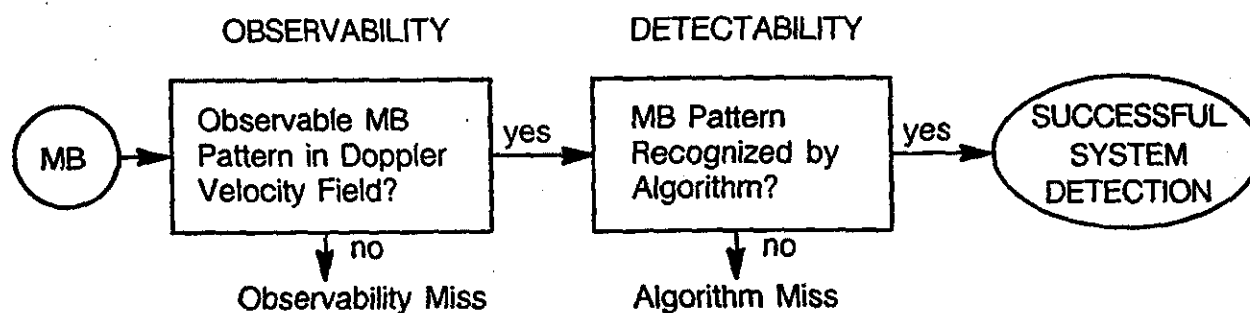
Figure I-1. *Relationship between microburst observability by radar and algorithm detectability, with respect to overall system performance.*

This report considers a number of potential limitations which may restrict the observability of microbursts by single–Doppler radar. They include:

(1) low signal–to–noise ratio (SNR) and/or signal–to–clutter ratio (SCR),
(2) unfavorable viewing angle of asymmetric microburst outflow,
(3) microburst outflow limited to a shallow depth (below radar beam), and
(4) radar beam blockage.

The effects of these limitations on the performance of microburst observability by radar are investigated, with an attempt to estimate the extent to which they are likely to decrease the overall system's probability of detection of microburst wind shear. This is done through a comparative analysis of Doppler radar data and data collected from a mesoscale network (mesonet) of surface weather sensors during 1988 in the vicinity of Denver, CO. Similar studies have been performed using data from Denver in 1987 (DiStefano, 1988), Huntsville, AL in 1986 (Clark, 1988), and Memphis, TN in 1985 (DiStefano, 1987). Results from 1988 are compared to previous results in Denver and Huntsville, for which the radar and surface data collection strategies were comparable.

Both the radar and surface data used for this study were collected as part of the FAA TDWR measurement program which during 1988 was sited at Denver,CO. Data was collected from 11 April to 13 September; this period included the TDWR Operational Demonstration which took place during the months of July and August at Denver's Stapleton International Airport. The radars used were an S–band radar (FL–2) developed and operated by Lincoln Laboratory for the FAA (Evans and Turnbull, 1985), and a C–band radar that was operated by the University of North Dakota (UND). The surface mesonet system consisted of 30 FAA–Lincoln Laboratory Operational Weather Studies (FLOWS) weather stations (Wolfson et al., 1987) and the 12–station enhanced Low Level Windshear Alert System (LLWAS) surrounding Stapleton International Airport. The FLOWS stations collected data on several meteorological parameters (barometric pressure, relative humidity, temperature, precipitation rate, average and peak wind speed and direction), while the LLWAS stations recorded only wind speed and direction. The locations of both radars and all surface weather stations with respect to the airport runways are shown in Figure I–2.

Chapter II of this report describes the methodology used in comparing radar and surface data in order to identify microbursts. Chapter III summarizes the results of the study, including observability percentages and microburst frequency for 1988, and comparison of results to previous microburst observability studies. Analyses of microbursts which were unobservable by single–Doppler radar are presented in Chapter IV. A summary is given in Chapter V, and a brief description of ongoing and future radar/surface data analysis is provided in Chapter VI.
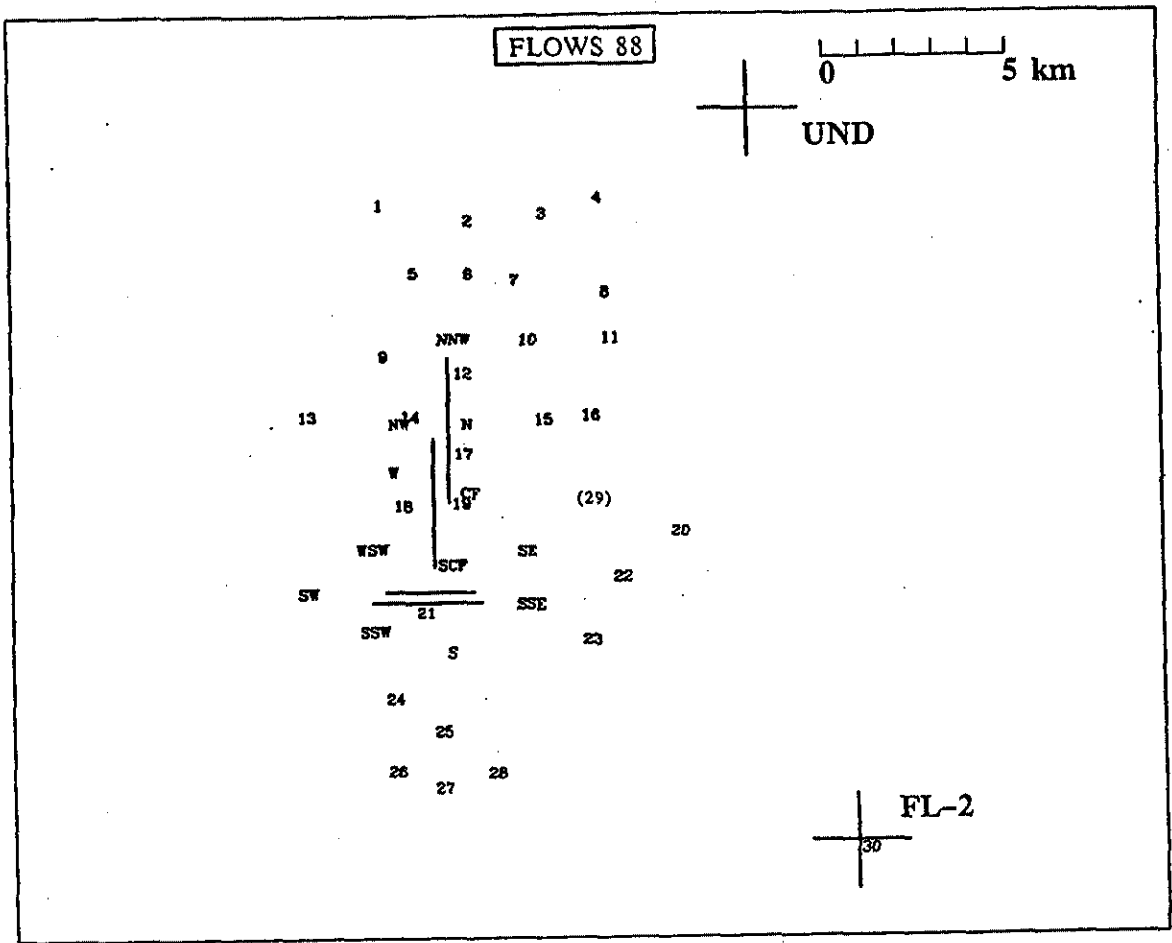
Figure I-2. *The 1988 surface mesonet layout in Denver, CO. FLOWS stations numbered 1 through 30. (Station #29, shown in parentheses, was not operable during 1988.) LLWAS stations are labelled with directional abbreviations. Radar locations are indicated by cross marks. The runways of Stapleton International Airport are denoted by straight lines in center of mesonet.*

II. METHODOLOGY USED IN IDENTIFYING MICROBURSTS

The observability of microbursts was determined through a comparison of surface weather data and Doppler weather radar data. The methodology was essentially the same as that used for previous microburst observability studies of data from Memphis in 1985 (DiStefano, 1987), Huntsville in 1986 (Clark, 1988), and Denver in 1987 (DiStefano, 1988). Surface and radar data were examined for the appearance of the horizontal divergence associated with microburst outflow, and a comparative analysis was performed on an event-by-event basis. A brief description of the microburst identification and comparison methodology follows.

A. Using Surface Mesonet Data

The surface sensor data for each station were converted to a common format for further processing as described in Wolfson et al. (1987). For each day of data, values of the various meteorological parameters were plotted on a 24-hour time series graph for each station. Each of these plots was examined for evidence of possible wind shear events, with the primary indicator being a sharp peak in wind speed at one or more stations, accompanied by a change in wind direction. Other indicators included an abrupt change in temperature, pressure, and/or relative humidity, as well as the occurrence of precipitation.

Several steps, involving both objective and subjective analysis, were then taken to investigate the potential wind shear events identified from the 24-hour plots. The most significant of these was identifying surface wind divergence associated with microburst outflow. This was done through examination of a series of one-minute mesoscale wind plots which depicted the surface wind field for the time period covering the potential event. An objective analysis scheme was used for computing the maximum velocity difference between all combinations of station pairs within a divergence area. In order for an event to be classified as a microburst, at least one pair of stations within the divergence area was required to exhibit a differential velocity of at least 10 m/s within a distance of 4 km. In instances where the maximum differential velocity was measured between stations separated by more than 4 km, it was also required that at least one pair of stations within the divergence area exhibit a horizontal shear of at least $2.5 \times 10^{-3} s^{-1}$, equivalent to a 10 m/s differential velocity across 4 km.

B. Using Doppler Radar Data

The microburst signature is identified in the Doppler velocity field as a divergent outflow at or near the ground, apparent as a couplet of approaching and receding radial velocities in the low-elevation radar scans. In order for a wind shear event to be classified as a microburst, it had to exhibit a velocity differential of at least 10 m/s within a horizontal range of no more than 4 km along a radial extending across the outflow area. This criterion provides a threshold similar to those used in operational microburst detection algorithms (Campbell and Merritt, 1987), although these algorithms also apply additional requirements

for spatial and temporal continuity (Merritt, 1987) and association with features aloft (Campbell, 1988).

In addition to the appearance of a divergence signature in the Doppler velocity field, the existence of a parent cloud from which the microburst could emanate (Fujita, 1985) was also necessary for classification as a microburst. This was evidenced by a cell of reflectivity associated with the surface divergence. Since a considerable portion of the microbursts in Denver are of the "dry" variety originating within very high cloud bases, it was often necessary to search higher-elevation radar scans in order to identify the parent cloud. There were some instances during 1988 when a surface divergence was slightly above threshold but not accompanied by a parent cloud, and was therefore not classified as a microburst.

The FL-2 radar, which provides a 0 dB SNR for -15 dBz at a range of 15 km, was used as the primary source of data for microburst identification by radar. However, UND radar data were used when FL-2 data were not available, or when a microburst that was identified in the surface mesonet data was not observable by FL-2. For each microburst, the time of maximum differential velocity observable in the Doppler velocity field was recorded, as well as the horizontal distance between the maximum approaching and receding velocities in the radar couplet.

C. Comparison of Radar and Mesonet Data

Microburst observability was determined through comparison of radar and mesonet data for microbursts identified within the mesonet area. Microbursts identified by the surface sensors were checked against the corresponding radar data; similarly, microbursts identified from radar data (including those identified and logged in both real-time and playback mode by radar operators) were compared with mesonet data. Upon comparison of data, each microburst was classified as either observable or unobservable by radar and mesonet based on the criteria described in the preceding sections. Incidentally, it was also possible for a wind shear event exhibiting microburst-strength divergence ultimately *not* to be classified as a microburst if, for instance, the surface divergence was not associated with a parent cloud identifiable in the radar reflectivity data. Such events are then disregarded with respect to the overall assessment of observability.

It is also worthy of note that the observability classification was determined on an event-by-event basis, i.e. each microburst was declared either observable or unobservable. This differs from many microburst "truthing" schemes for assessment of detection algorithm performance, which determine microburst detection on a minute-by-minute basis such that a single microburst could include both "detectable" and "undetectable" minutes. This distinction is important to understand when comparing microburst observability by radar with performance assessment of microburst pattern-recognition algorithms.

- 6 -

III. SUMMARY OF RESULTS

A. Microburst Observability and Frequency

A total of 184 microbursts were identified which impacted the surface mesonet area during the data collection period of 11 April to 13 September 1988. Of these, there were 155 microbursts for which both FL-2 radar and surface data were available for comparison. There were also two other microbursts for which radar data were available from UND only; for consistency, these two events were excluded from the observability statistics since UND's data quality and clutter suppression capabilities are notably inferior to that of FL-2. Table III-1 presents a summary of identified microbursts, including an observability break-down categorized by strength; a complete detailed listing of all microbursts identified in this study is provided in Appendix A.

Table III-1. *Categorization of 1988 Microburst Observability by Strength*

(Strength determined by Maximum Velocity Difference measured by FL-2 radar for those observed by the radar, and Maximum Velocity Difference measured by surface sensors for others.)

	Weak			Strong	All
	10-14m/s	15-19m/s	All	20+ m/s	Total
Total Microbursts (MB) Identified	70(38%)	58(32%)	128(70%)	56(30%)	184
MB with available FL-2 & surface data	61(40%)	47(30%)	108(70%)	47(30%)	155
MB for which FL-2 data not available	9(31%)	11(38%)	20(69%)	9(31%)	29
For MB with available FL-2 & surface data:					
MB observable by FL-2 radar	59(97%)	47(100%)	106(98%)	45(96%)	151(97%)
MB observable by mesonet	54(89%)	44(94%)	98(91%)	47(100%)	145(94%)
MB observed by both FL-2 and mesonet	52(85%)	44(94%)	96(89%)	45(96%)	141(91%)

Table III-1 shows that 151 of 155 (97%) microbursts were observable by radar. In contrast to other microburst observability studies [DiStefano, 1988; Clark, 1988], observability by radar was actually slightly greater for weak microbursts than for strong microbursts. Contributing to this result was the fact that all 47 weak microbursts with maximum differential velocities ranging from 15 to 19 m/s were observable. The weak microbursts that were unobservable by radar exhibited maximum differential velocities below 15 m/s; microbursts of this strength are generally considered to pose little or no threat to aircraft safety. Incidentally, a considerable portion (38%) of the microbursts identified during 1988 attained a maximum velocity difference of less than 15 m/s.

The observability percentage of the strong microbursts was reduced by the two strong events which occurred on 27 May and 2 July. One was unobservable due to low SNR and/or low SCR, while the other was due to an asymmetric outflow with low SNR and/or low SCR

also a contributing factor. In Denver (and presumably in all dry environments), there appears to be little correlation between microburst strength and radar echo intensity (Wilson et al., 1984). Consequently, one might expect low SNR to impact the observability of both weak and strong events, as was the case during 1987 in Denver (DiStefano, 1988). However, on an event by event basis in 1988, the observability of only two microbursts (both categorized as strong) were affected by low SNR. This is somewhat misleading, for although the event on 27 May went unobserved entirely as a result of low SNR, this was not the case for the 2 July event. As previously indicated, both asymmetry and low SNR (and/or low SCR) contributed to this event being unobserved by radar. Asymmetry was the contributing factor while this microburst was in its strong phase, and low SNR/SCR was the contributing factor during the weak phase. So, in actuality, the observability of both a weak and strong event were affected by low SNR during 1988.

In contrast to the impact of low SNR on observability, the effects of asymmetric or shallow outflow, which tend to cause an underestimate of surface divergence, are more pronounced on observability of weaker events since an underestimate of their magnitude is more likely to bring them below some microburst–strength threshold. In wetter environments such as Huntsville where low SNR/SCR does not appear to be a problem for observability, one would expect more of a distinction between observability of weak and strong microbursts. Although this difference is not expected to be as apparent in Denver, it is still expected to some degree for a large sample size, and the reverse relationship seen in 1988 is considered an anomaly.

There were four microbursts which were classified as unobservable by FL–2 radar. Two of these were categorized as weak and two as strong, as determined by the maximum velocity difference measured by the surface mesonet. As mentioned, one of the strong events was unobservable due to low SNR and/or low SCR, while the other was due to asymmetry with low SNR and/or low SCR also a contributing factor. As for the weak microbursts, one was unobserved due to a shallow outflow, while the other was unobserved due to asymmetry. A summary of these four microbursts is listed in Table III–2; the table identifies the time period during which divergence was apparent in the surface wind field, and the maximum velocity differential observed by the mesonet. The circumstances surrounding these events are described in detail in Section IV. In addition, there was one other microburst which was unobservable by UND due to low SNR; it is not included here because no FL–2 data were available for the event.

Table III–3 compares 1988 microburst frequency and observability with results of similar studies of data from Denver in 1987 and Huntsville, AL in 1986 [Clark and DiStefano, 1989]. The table is divided into two parts: Part A is a summary of all microbursts with available radar and mesonet data, while Part B shows a comparison which includes only the data collection period of 6 June – 13 September, which was common to all three years. First comparing the two years in Denver, the table shows an increase in microburst observability

Table III-2.	*1988 Microbursts Unobservable by Radar*			
MB #	DATE	TIME(UTC)	MAX ΔV	EXPLANATION
45	26 May	2035–2041	14	Shallow Outflow
52	27 May	2100–2120	30	Low SNR
101	2 July	2211–2225	21	Asymmetry/Low SNR
139	17 July	0024–0034	14	Asymmetry

by radar from 94% in 1987 to 97% in 1988. There was also a large increase in microburst frequency in 1988 (50% more microbursts per Data Collection Day). However, since Microburst Days occurred with similar frequency for the two years (25% of the days in 1987, 28% in 1988), the difference was primarily due to the large increase in microburst frequency *per Microburst Day* (up from 3.3 to 4.3 microbursts per Microburst Day). This fact is weighed heavily by a number of "frantic" microburst days in 1988: 12 microbursts occurred on 9 June, 17 occurred on 16 July, and 14 on 9 August. This difference is even more marked during the "common" data collection period (Table III-3B); there were two fewer Microburst Days in 1988 with 27 more microbursts, corresponding to nearly 40% more microbursts per Microburst Day.

Table III-3. *Comparison of Annual Microburst Frequency and Observability*

(A)

Year/Site	Data Period	Total MB	MB/ Day	MB Days	MB/ MB Day	Observability by Radar: Weak	Strong	All
1986 Huntsville	3 Apr–9 Dec	131	0.5	39 (16%)	3.4	98%	100%	98%
1987 Denver	6 Jun–5 Oct	102	0.8	31 (25%)	3.3	91%	97%	94%
1988 Denver	11 Apr–13 Sep	184	1.2	43 (28%)	4.3	98%	96%	97%
TOTAL		417	0.8	113 (21%)	3.7	97%	97%	97%

(B)

Year/Site	Data Period	Total MB	MB/ Day	MB Days	MB/ MB Day
1986 Huntsville	6 Jun–13 Sep	98	1.0	24 (24%)	4.1
1987 Denver	6 Jun–13 Sep	99	1.0	29 (29%)	3.4
1988 Denver	6 Jun–13 Sep	127	1.3	27 (27%)	4.7

Comparison of data from Denver and Huntsville shows a slightly greater microburst observability by radar in Huntsville. Low signal-to-noise ratio that resulted in several unob-

servable microbursts in Denver did not pose a problem in the wetter Huntsville environment, and this appears to account for the difference in observability between the two sites. Comparing the microburst frequency at the two sites must be approached with more caution, since the Huntsville mesonet was comprised of more stations covering a much larger area (see Table III–4 for mesonet characteristics). The data collection during 1986 also extended well past the "microburst season", and included the less active months of October–December, which contributed to the lesser percentage of Microburst Days occurring in Huntsville (Table III–3A.) This factor is eliminated in Part B of Table III which includes only the com-

Table III–4. *Characteristics of the Huntsville and Denver mesonets.*

	HUNTSVILLE, 1986		DENVER 1987/1988
	Standard	Expanded *	
Number of Surface Stations	36	77	42
Coverage Area (sq. km)	500	1000	150
Avg station spacing (km)	3–5	1–4 **	2–2.5
Max range from radar (km)	22	31	22

* The mesonet was expanded during June and July with the inclusion of NCAR's Portable Automated Mesonet (PAM) *stations.*

** Beyond 20 km radius from the radar, station spacing was 4–8 km

mon data collection period. In spite of the larger mesonet area in Huntsville, the number of microbursts identified during the common period was still somewhat less than that found in Denver, indicating the Denver frequency of microburst *per unit area* to be considerably greater. Once again, this difference is likely due to the significant proportion of "dry" Denver microbursts, the occurrence of which is most favorable in the High Plains environment.

B. Monthly and Diurnal Variation

Table III–5 presents a monthly breakdown of microburst frequency for all microbursts identified during the three data collection years 1986–1988. For each year, the table shows the number of Microburst Days occurring during each month, the percentage of Microburst Days based on data collection days during that month, and the total number of microbursts identified. The data for 1988 also indicates the number of strong microbursts (at least 20 m/s velocity difference) identified for each month. For all three years, the greatest number of microbursts occurred during June and July, with August also showing a relatively high microburst frequency in 1986 and 1988 in spite of considerably fewer Microburst Days. Also of note is the high frequency of microbursts in April of 1988: during only twenty days of data collection, a total of 27 microbursts were identified with microbursts occurring on 40% of the days. Extrapolated to a full month of data collection, the microburst total for April rivals that of June and July. Unfortunately, there is no corresponding April data from Den-

Table III-5. *Monthly Variation of Microburst Frequency*

| | Denver 1988 | | | Denver 1987 | | Huntsville 1986 | |
	MB Days (%)	MB	[Strong]	MB Days (%)	MB	MB Days (%)	MB
April	8 (40%)	27	[3]	–	–	1 (4%)	1
May	8 (26%)	26	[6]	–	–	2 (6%)	3
June	10 (33%)	45	[9]	10 (40%)	34	9 (30%)	32
July	10 (32%)	49	[24]	11 (35%)	31	10 (32%)	44
August	6 (19%)	30	[14]	6 (19%)	11	8 (26%)	31
September	1 (8%)	7	[0]	4 (13%)	26	4 (13%)	13
October	–	–	–	0 (0%)	0	2 (6%)	3
November	–	–	–	–	–	3 (10%)	4
December	–	–	–	–	–	0 (0%)	0

ver 1987 for comparison, so it is not known whether the high frequency was simply a one-year anomaly. There was certainly no evidence of this high April frequency in Huntsville 1986, as only one microburst was identified during 28 data collection days. Furthermore, when considering only strong microbursts, the 1988 monthly frequency distribution appears to be more Gaussian, peaking in July and showing no anomalously high frequency in April. (Note that the occurrence of strong microbursts as a percentage of total microbursts is much greater, nearly 50%, for July and August than for the other months.) A comparison of Denver and Huntsville data (keeping in mind the difference in mesonet areal coverage) shows reasonable similarity in percentage of Microburst Days and microburst frequency for June through September, with far fewer microbursts identified in Huntsville during the spring months.

The diurnal distribution of all microbursts occurring during 1988 in Denver is shown in Figure III-1. The most common hour for microburst occurrence was 4–5 PM Local Daylight Time, during which time 22% of the microbursts reached their maximum differential velocity. More than half of the microbursts occurred from 2–5 PM, and 80% occurred between 1–7 PM. No microbursts were identified between 11 PM and 12 Noon. Inspection of only strong microbursts yields a similar distribution, with a secondary relative maximum occurring between 1–2 PM.

C. Comparison of Maximum Differential Velocity as Measured by Radar and Mesonet

The magnitude and time of occurrence of maximum differential velocity (MaxΔV) attained by each microburst were recorded from measurements of both radar and surface
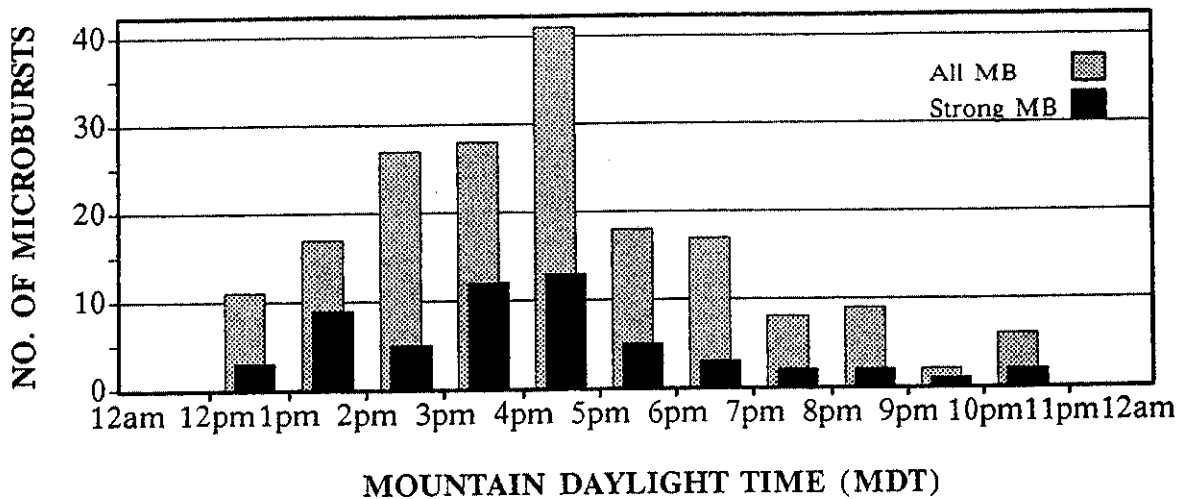
Figure III-1. *Diurnal Frequency Distribution of 1988 Denver Microbursts.*

data. (This information is included in the detailed microburst listing, Appendix A.) Measurements by radar and mesonet were compared in order to consider the typical time evolution of microburst development, as well as to comparatively examine the measurements yielded by the two different sensing systems. A subset of microbursts was used for this comparison; the subset included the 141 microbursts which were observable by both radar and mesonet, and for which complete data were available from both sensing systems. (There was one microburst observable by radar and mesonet for which radar scans were missing at the onset of the event; this event was excluded from the analysis.) The radar/mesonet comparison of MaxΔV for this subset is summarized in Table III-6.

Perhaps the more significant aspect of this comparison involved the time of occurrence of MaxΔV as measured by radar and mesonet. On average, MaxΔV as measured by radar was attained approximately one minute prior to that as measured by the surface sensors. There were nearly twice as many microbursts for which MaxΔV occurred first aloft, measured by the radar's lowest elevation scan, than at the surface. When the timing was considerably different, i.e. when MaxΔV differed by at least two minutes, the radar MaxΔV measurement occurred prior to that of the surface mesonet measurement of MaxΔV approximately two and one-half times more frequently than it occurred "later". For about one-third of the events, the time of MaxΔV measured by radar and mesonet differed by no more than one minute.

The data implies that sensing by radar, i.e. examining the wind environment up to a few hundred meters above ground level, may afford more timely (perhaps on the order of one minute) detection of wind shear development than does surface sensor measurements. Implicit is the assumption that the radar/mesonet relationship of MaxΔV timing is similar to the timing with which the two sensing systems would initially attain some "microburst threshold" measurement. A plot of ΔV-vs.-Time for radar and mesonet would be expected

- 12 -

Table III-6. *Comparison of Max ΔV Measured by Radar and Mesonet*

A. Max ΔV Time Comparison

No. of times radar Max ΔV occurred first	81	57%
No. of times mesonet Max ΔV occurred first	43	31%
No. of times radar/mesonet Max ΔV occurred same minute	17	12%
No. of times radar Max ΔV occurred at least 2 min. earlier	65	46%
No. of times mesonet Max ΔV occurred at least 2 min. earlier	27	19%
No. of times radar/mesonet Max ΔV occurred within 1 min.	49	35%

B. Max ΔV Magnitude Comparison

No. of times radar Max ΔV was greater	45	32%
No. of times mesonet Max ΔV was greater	85	60%
No. of times radar/mesonet Max ΔV were same	11	8%
No. of times radar Max ΔV was more than 5 m/s greater	4	3%
No. of times mesonet Max ΔV was more than 5 m/s greater	32	23%
No. of times radar/mesonet Max ΔV were within 5 m/s	105	74%

to yield two similarly-shaped curves differing by some time lag (Fig. III-2A), rather than, say, curves of different periods in which a threshold measurement is first attained by mesonet, yet with the maximum amplitude of the mesonet lagging behind that of the radar (Fig. III-2B). Experience of the authors is that the former is a more typical radar/mesonet

Figure III-2. *Schematic examples showing possible relationship between radar and mesonet measurement of differential velocity as a function of time, showing curves of (A) same and (B) differing periodicity.*
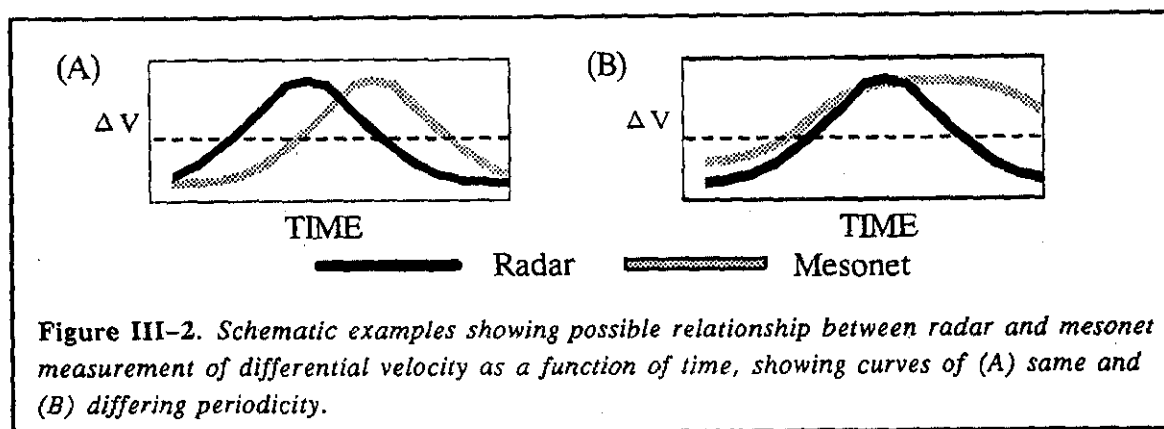
timing relationship. As an example, a plot of ΔV-vs.-Time as measured by both radar and mesonet for a microburst occurring on 9 June 1988 is shown in Figure III-3. This microburst was selected because it developed and remained entirely within the mesonet in an area of dense station coverage. It shows MaxΔV (radar) attained at 2148 UTC, with MaxΔV (mesonet) occurring three minutes later. The microburst threshold is also attained earlier by radar, at 2143 UTC. This threshold is first reached by the mesonet at 2144 UTC; the velocity

- 13 -

differential then drops below threshold for a couple of minutes and reaches threshold again between 2146 and 2147 UTC.

Figure III-3. *Differential Velocity-vs.-Time as measured by radar and surface mesonet for microburst occuring on 9 June 1988.*
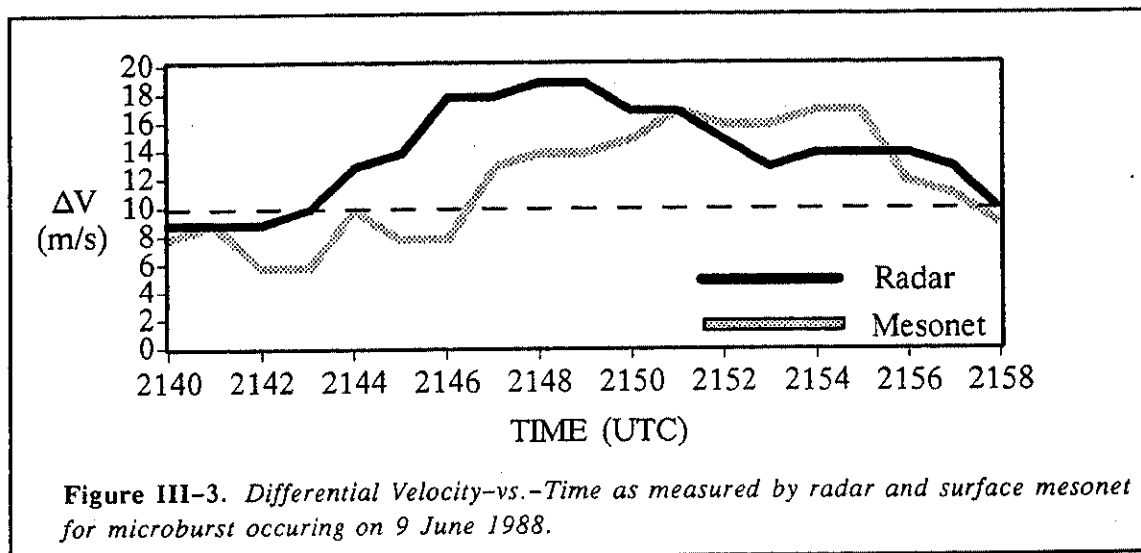
The magnitude of MaxΔV measured by radar were also compared (refer back to Table III-6B). MaxΔV as measured by mesonet was typically higher than that of radar, and this relationship was increasingly evident for microbursts with larger mesonet/radar differences. On average, the mesonet measurement of MaxΔV was 2 m/s greater than that of radar, a difference of a little more than 10%. One might expect a greater wind divergence at the surface as the downward momentum of the microburst is transferred into the horizontal as it impacts the ground. Consideration must also be given, however, to the differing measurement characteristics of the two sensors: the radar velocity measurements are high spatial resolution volume averages of radial components, whereas the surface mesonet yields relatively low spatial resolution point measurements of the total wind vector. These differences may contribute to any difference in comparisons of Max ΔV. Also, the asymmetric geometry common in microburst outflow would also have a greater impact in underestimating MaxΔV by radar; however, Clark (1988) has suggested that this effect, on average for a large number of events, is reasonably compensated by the superior spatial resolution of the radar measurements.

The data presented here provides a limited insight into both the timing and wind speed estimate relationships of radar and surface sensing; a more comprehensive analysis of numerous examples, beyond the scope of this report, is required to substantiate these implications. A clearer understanding of the radar/surface wind measurement relationship will be most valuable in developing an integrated wind shear warning system which incorporates both the Doppler velocity data provided by TDWR and surface wind information available from the LLWAS surface network.

IV. MICROBURSTS UNOBSERVABLE BY RADAR

During the 1988 TDWR Project in Denver, there were four microburst events that were unobservable by the FL-2 radar. This represented 2.6% of the events for which both radar and surface data were available. As mentioned in the previous chapter, two of these events were categorized as strong microbursts (MaxΔV > 20 m/s), while the other two were weak, exhibiting maximum differential velocities of less than 15 m/s. Following is a brief synopsis of each case.

A. Case 1: 26 May 1988 (2035-2041 UTC)

The microburst, which impacted the north/south runways at Denver's Stapleton Airport on 26 May, was clearly identified by the surface mesonet sensors. Figure IV-1 shows this microburst when it was positioned directly over the north/south runways at 2038 UTC at a range of approximately 16 km from FL-2. Shear calculations performed on this microburst yielded results which categorized the event as weak. Figure IV-2 shows that the maximum velocity differential remained below 15 m/s for the duration of the event.

Figure IV-1. *Mesonet plot showing the surface wind field on 26 May 1988 at 2038 UTC. Dashed line indicates microburst divergent outflow area. Full barb represents 5 m/s and half-barb 2.5 m/s.*

Figure IV-2. *Maximum differential velocity as computed from mesonet data for microburst on 26 May 1988 from 2035-2041 UTC.*

According to radar data collected by FL-2, the cell responsible for this event was visible at tilts just above the lowest-level surface scan. However, in the vicinity of the event, neither the FL-2 nor the UND radar observed microburst strength ΔV's (i.e. ≥ 10 m/s over a distance not greater than 4 km). Some weak divergence was indicated. However, maximum ΔV's reached only 5-7 m/s.

Apparently, the microburst strength outflow from this event was shallow in depth and located close to the surface. The microburst occurred in a location where distance from the radar, local topography (sloping downward with increasing range from FL-2), and antenna tilt angle (0.4°) all resulted in a layer at the surface more than 100 m deep where the radar's main lobe did not scan. According to Wilson et al. (1984), 75 m AGL is the height where maximum differential velocities associated with microbursts occur. The fact that:

> (1) this height (75 m) lies safely within the 100 m surface layer not scanned by the radar,
> (2) the mesonet surface sensors clearly identified this event, and
> (3) adequate SNR was indicated,

all support the assumption that this microburst was not observed by radar because its outflow was shallow in depth and located close to the surface.

Similar analyses were performed on a microburst that occurred in Denver on 2 September 1987, to determine if a shallow outflow was the reason radar did not observe the event (see DiStefano, 1988, pp. 79-82). It was shown by simulating the wind profile with height between the the lowest antenna tilt angle and the surface, that a closer estimate to the maximum velocity differential, as observed at the surface, could be attained. These results

suggested that by adjusting the antenna tilt angle lower, a better representation of the microburst wind shear could have been measured. However, in doing this, the probability of encountering high level ground clutter due to increased main lobe illumination of ground clutter targets would increase. Therefore, a microburst having this particular signature at this location could not effectively be observed.

B.   Case 2:   27 May 1988 (2100–2120 UTC)

The second of two microbursts which impacted the mesonet on 27 May 1988 occurred in the northern portion of the network during the period 2100–2120 UTC. By 2112 UTC, this event was affecting the entire northern third of the mesonet (see Figure IV–3). Velocity differentials as measured by the mesonet surface stations for this microburst peaked at 30 m/s and remained above 20 m/s for more than 10 minutes. Figure IV–4 shows the Max ΔV trace for this microburst which was categorized as strong.

During this event, both the FL–2 and UND radars were operating. The cell which produced this microburst was not observed in the lowest surface scan by FL–2. The reflectivity
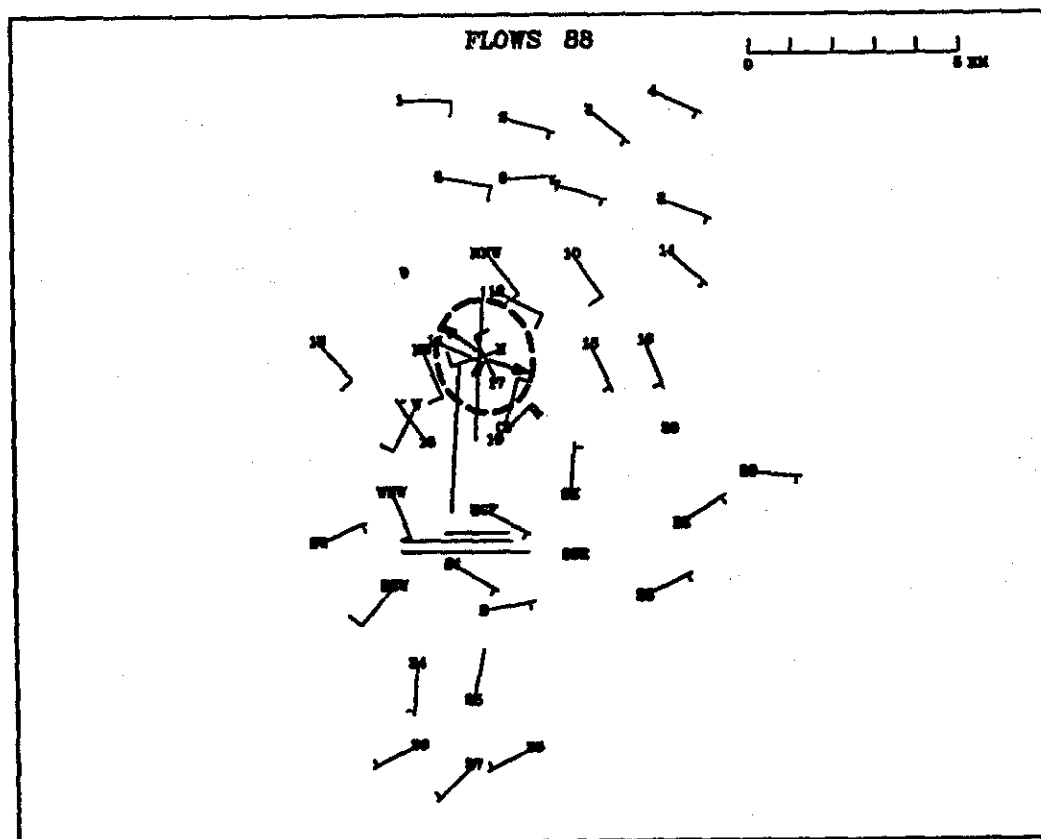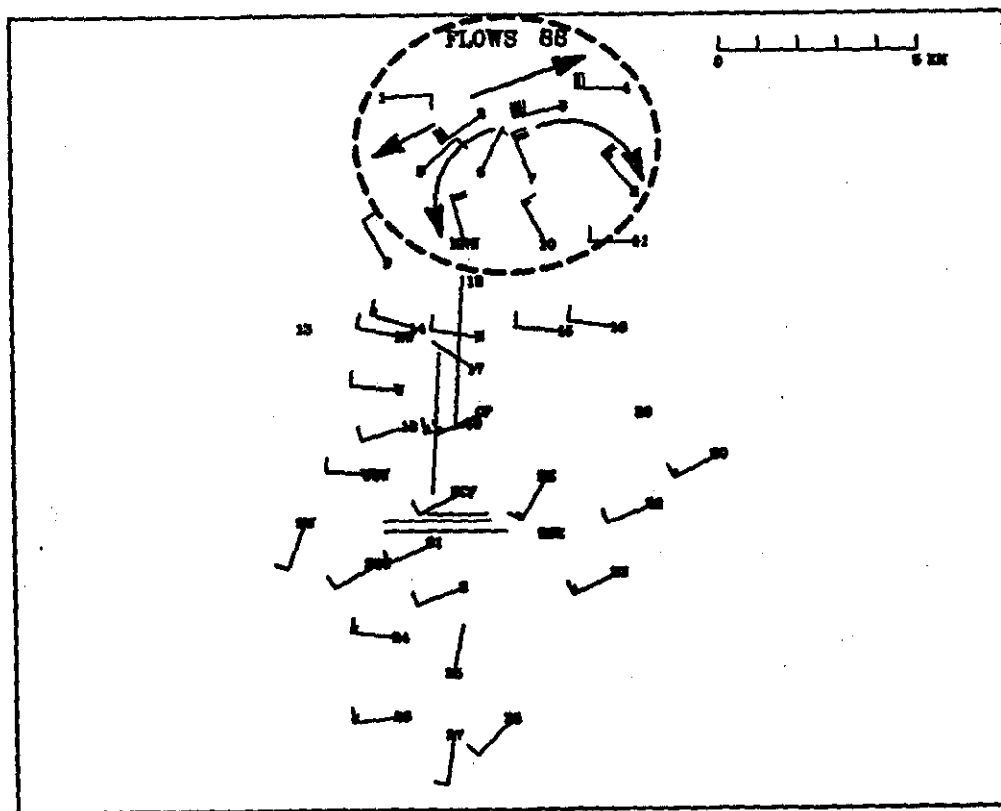

Figure IV-3. *Mesonet plot showing the surface wind field on 27 May 1988 at 2112 UTC. Dashed line indicates microburst divergent outflow area. Full barb represents 5 m/s and half-barb 2.5 m/s.*
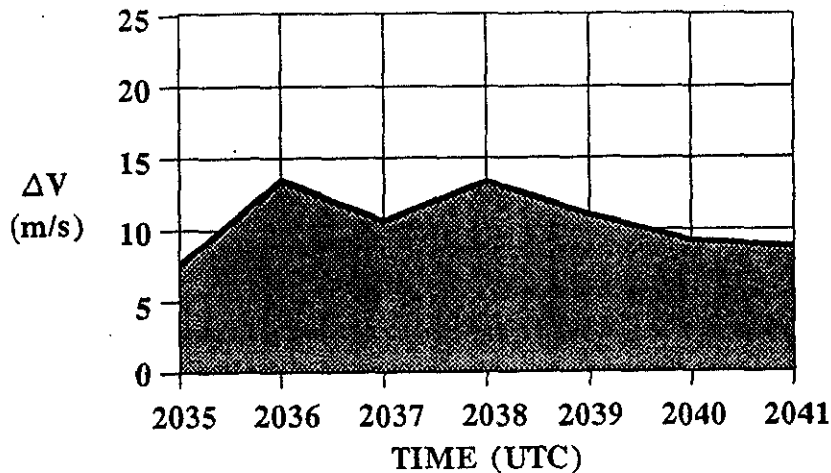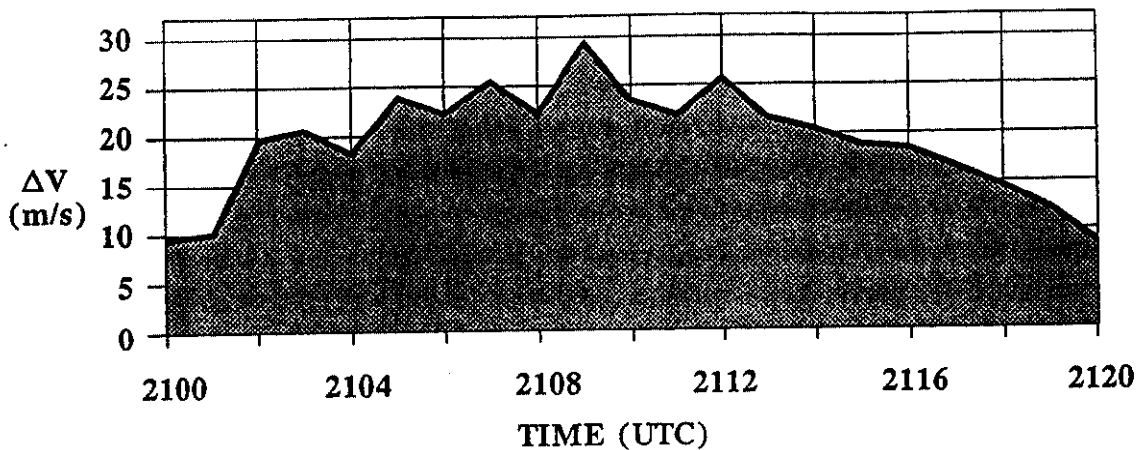
Figure IV-4. *Maximum differential velocity as computed from mesonet data for microburst on 27 May 1988 from 2100-2120 UTC.*

field from the low–elevation scan, thresholded at –1 dB, showed a maximum value of 5 dBz in the microburst–producing cell, with nominal clear–air values of –10 to –20 dBz away from the microburst area. Looking aloft, above the 2° elevation angle, the cell was apparent with maximum reflectivity values on the order of 20 dBz. With the SNR thresholded at 6 dB so that only the stronger signal in the vicinity of the event could be observed, FL–2's low–elevation Doppler field revealed velocity differentials that just barely exceeded threshold (10–11 m/s), and this during only two low–level scans (2059 and 2102 UTC). Apart from this, no distinguishable divergence at all was observed, and this as a direct result of low SNR. Even when divergence was observed by FL–2, the maximum radial distance over which this divergence was seen was less than 1.5 km (i.e., there was only a relatively small area where the SNR was greater than 6 dB). Divergence, as distinguished from the surface wind field measurements, however, was observed over a distance greater than 5 km. It should also be mentioned that because of low SNR, UND's radar was also not able to observe the event.

Further analysis showed that asymmetry was not a contributing factor which led to this microburst going unobserved by either radar. Inspection of radial wind components computed from mesonet and LLWAS surface winds indicated that strong divergence signatures should have been observable from both radars.

C. Case 3: 2 July 1988 (2211–2225 UTC)

·Five microbursts impacted the mesonet on 2 July. One of these events, which occurred in the northern sector of the mesonet between 2211 and 2225 UTC, was observed by the surface mesonet stations and the UND radar, but was missed by FL–2. It was a dry microburst

event as indicated by FL-2's surface reflectivity data from 2213 UTC; Figure IV-5 shows the areas of weak echo over the mesonet at that time. Maximum surface reflectivity associated with this microburst reached only 15 dBz and could be seen in the vicinity of station #2.

In the Doppler velocity field, with the SNR threshold at 6 dB, the UND radar was able to observe the divergence signature produced by this microburst which impacted the northwest portion of the mesonet (see Figure IV-6). At this time (2213 UTC), the area impacted by this microburst was represented by SNR values from both radars that were comfortably above the 6 dB threshold. FL-2, however, did not observe a microburst signature with this event but instead identified mainly rotation with only some weak divergence. A plot displaying the dual-Doppler wind field during this time portrayed a complex wind pattern over the mesonet. Figure IV-7 shows the dominant feature to be a divergent line extending southwest-northeast into the northern portion of the mesonet. A strong microburst was located on this line just west of Stapleton's runways. The microburst, which was not observed by FL-2, can be seen in this plot over the northern portion of the network. A divergent line extends west/east just north of station #1 and then southeastward into the northern portion of the mesonet. Associated with this line are two microbursts. One is located just north of the mesonet where the divergent line begins to bend southeastward, while the other, which is the event missed by FL-2, can be seen near mesonet stations #2, #6, and #7. The divergent flow associated with this microburst is notably asymmetric with the main axis of divergence aligned southwest-northeast which is in effect quasi-perpendicular to the beam's (FL-2's) main lobe.

The divergence signature associated with this microburst was identified by the mesonet surface stations during analysis of the wind field. Figure IV-8 shows that during this time, most of the network experienced strong west-northwesterly flow while the north-central portion of the mesonet was being affected by this microburst. The southeasterly flow at station #1 was associated with an anticyclonic vortex which was visible in the dual-Doppler plot in Figure IV-7. According to the surface data, the maximum velocity differential exceeded 21 m/s, thus allowing this event to be categorized as strong (see Figure IV-9).

Shortly after the surface divergence reached its peak strength, the typical SNR values associated with this event dropped considerably, from greater than 6 dB at 2213 UTC to approximately -2 dB at 2216 UTC, at which time neither FL-2 nor UND was able to observe the event despite continued microburst-strength divergence in the surface wind field. Consequently, the effects of both asymmetry, which was observed during the event's strong phase ($\Delta V \geq 20$ m/s), and low SNR, which was observed during the weak phase ($\Delta V < 20$ m/s), are considered contributors to the unobservability of this microburst.
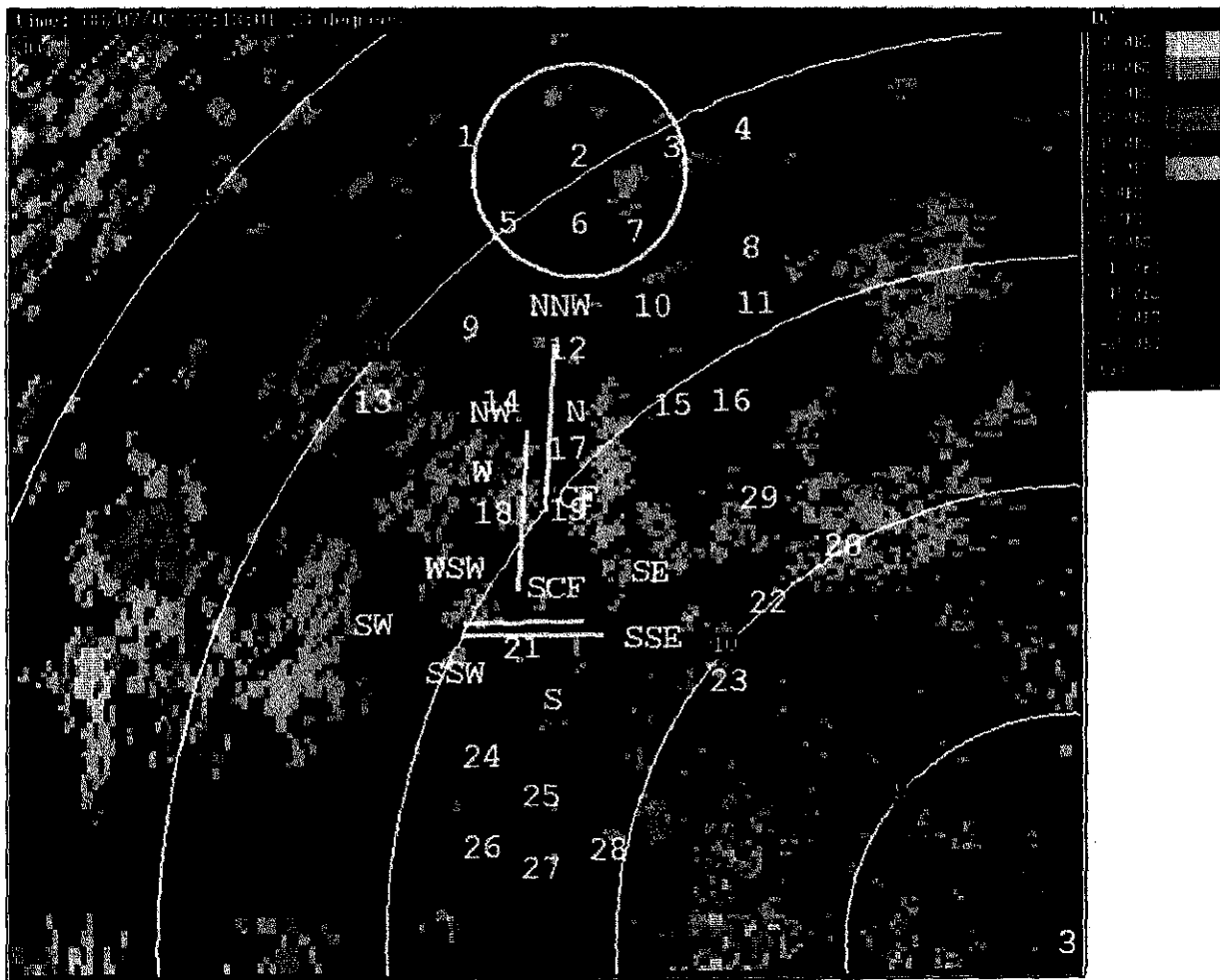
Figure IV-5. *FL-2 reflectivity field for 2 July 1988 at 2213 UTC. Cell that produced the microburst is identified within the white circle in the northern portion of the mesonet. Elevation angle is 0.3°. Range rings are every 5 km and locations of mesonet stations and airport runways are overlaid.*

Figure IV-6. *UND Doppler velocity field for 2 July 1988 at 2213 UTC. Microburst signature is located within the circle in the north portion of the mesonet. Elevation angle is 0.4 °. Range rings are every 5 km and locations of mesonet stations and airport runways are overlaid.*
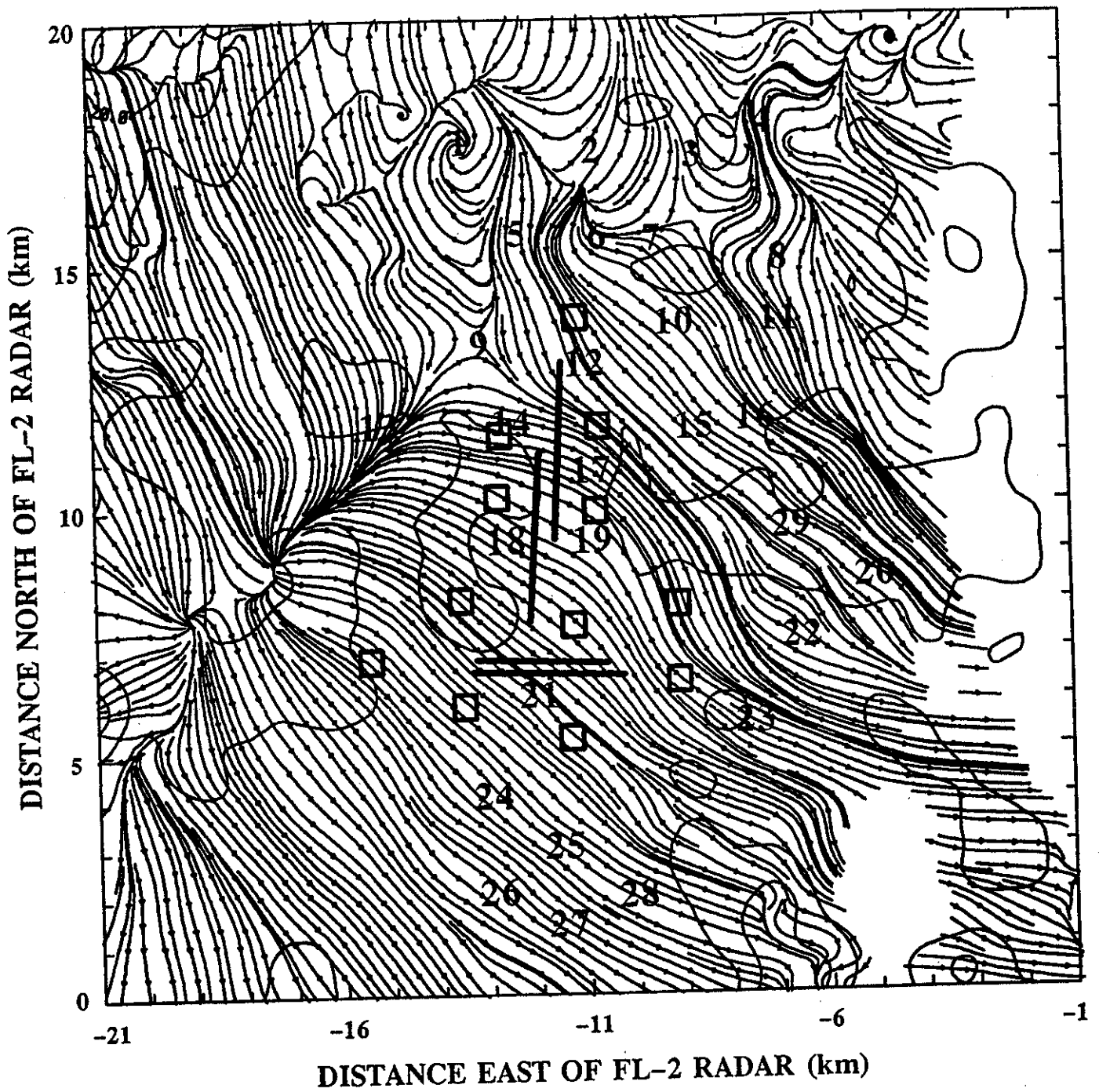
Figure IV-7. *Streamline analysis representing dual Doppler surface windfield for 2 July 1988 at 2212 (UTC). FL-2 and UND radars were used to generate this field. Airport runways and mesonet stations are overlaid. Small squares identify locations of LLWAS stations.*
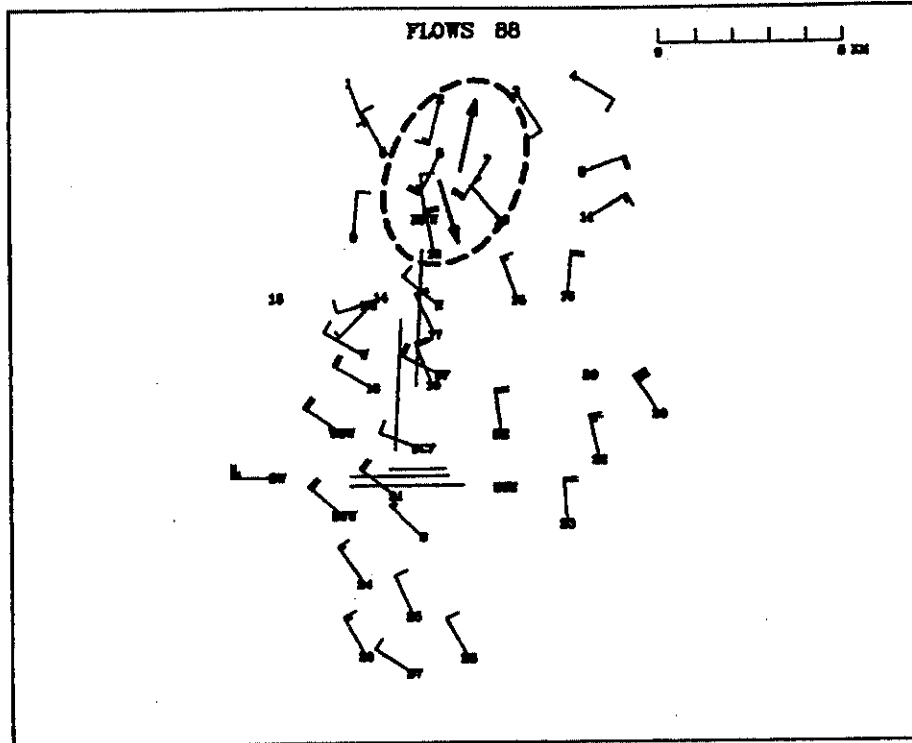
Figure IV-8. *Mesonet plot showing the surface wind field on 2 July 1988 at 2213 UTC. Dashed line indicates microburst divergent outflow area. Full barb represents 5 m/s and half-barb 2.5 m/s.*
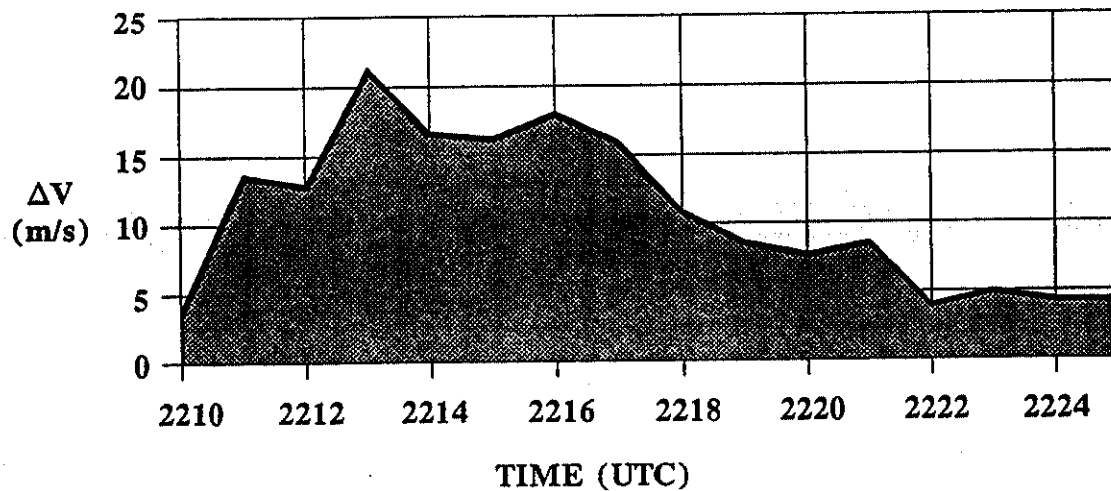
Figure IV-9. *Maximum differential velocity as computed from mesonet data for microburst on 2 July 1988 from 2210–2225 UTC.*

D. Case 4: 17 July 1988 (0024–0034 UTC)

A weak microburst was located in the northern portion of the mesonet along a divergence line which ran north to south, bisecting the northern half of the network. As seen in Figure IV–10, the surface wind field clearly identifies this event. Figure IV–11 indicates that the maximum velocity differential, as sensed by the surface mesonet stations for this microburst, reached 14 m/s.

The UND radar clearly identified this divergence line and associated microburst (surface reflectivities were observed between 25–30 dBz). At 0027 UTC, UND's Doppler velocity field indicated a 16 m/s velocity differential across the microburst (see Figure IV–12). According to the UND data, it was at this time that the microburst was strongest. FL-2, however, did not observe any microburst signature with this event. This was not surprising, since the wind field as depicted by the surface mesonet showed mainly a southerly component in the north–central portion of the net, and one would expect to see in this area only receding velocities. Profiles of Doppler radial velocities from FL-2 showed exactly that.
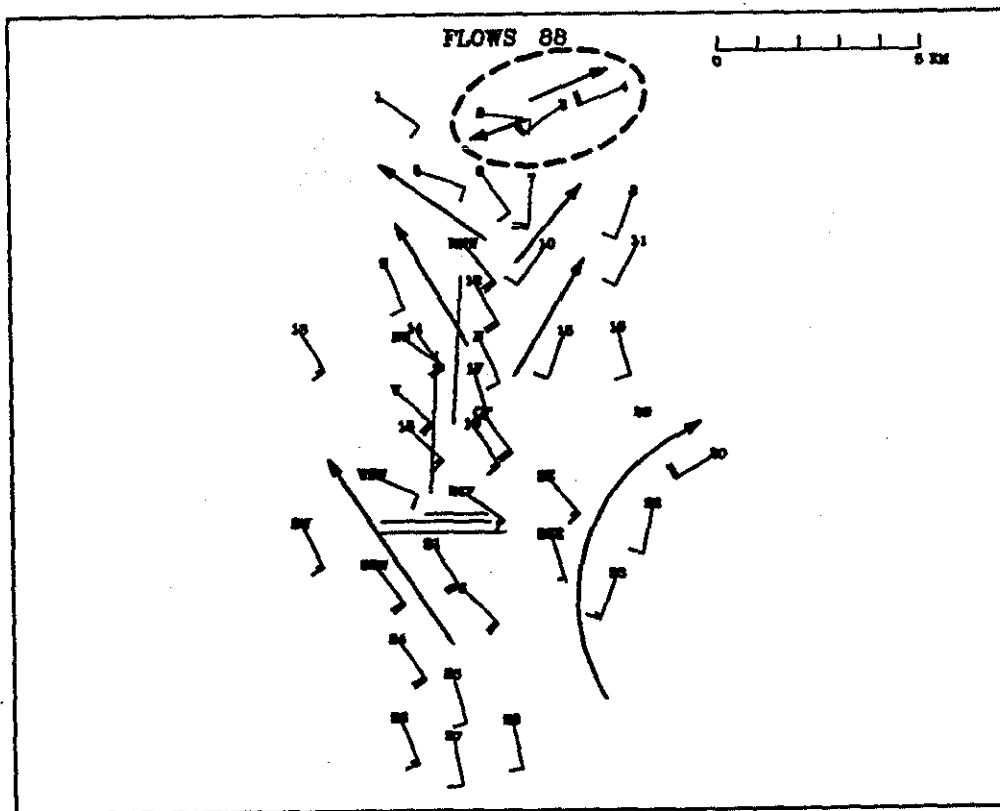
Figure IV-10. *Mesonet plot showing the surface wind field on 17 July 1988 at 0029 UTC. Dashed line indicates microburst divergent outflow area. Full barb represents 5 m/s and half–barb 2.5 m/s.*
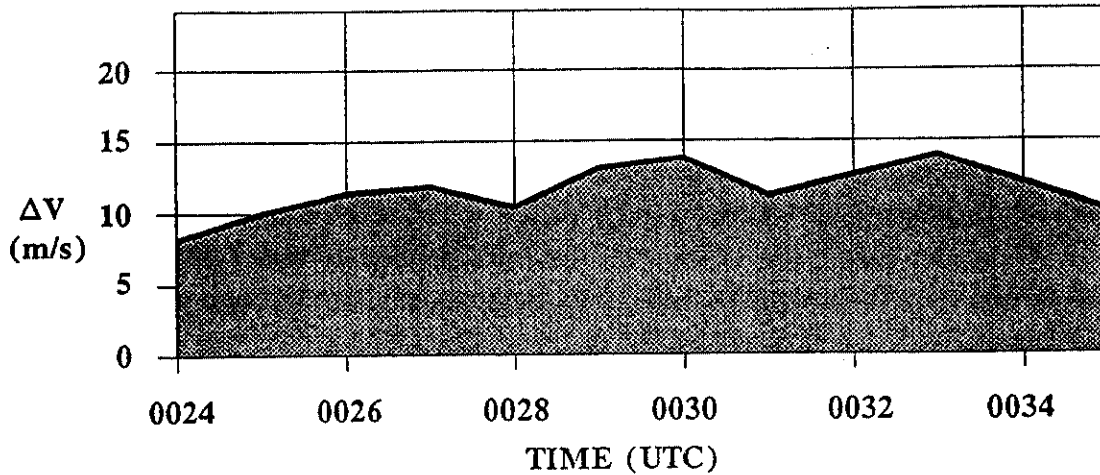
Figure IV-11. *Maximum differential velocity as computed from mesonet data for microburst on 17 July 1988 from 0024–0035 UTC.*

This microburst was not observed by FL-2 due to its asymmetric outflow. Measurements made using the radial wind components with respect to FL-2 and UND, and from the mesonet and LLWAS surface sensors confirmed this result. A clear microburst divergent signature was observed from the vantage point of UND, whereas only very weak divergence (well below microburst threshold) was seen from the viewing angle of FL-2.
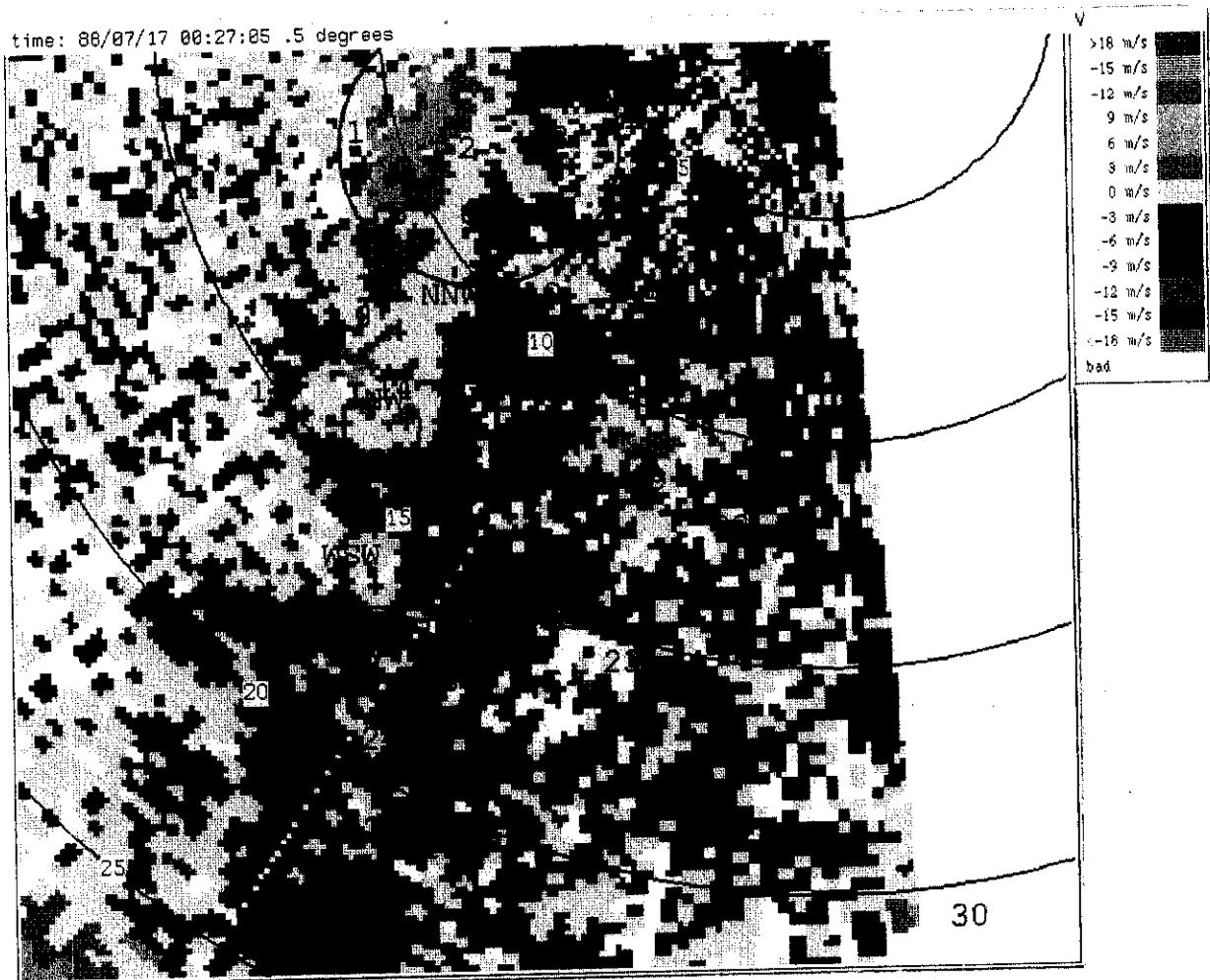
Figure IV-12. *UND Doppler velocity field for 17 July 1988 at 0027 UTC. Microburst signature is located within the circle in the northern portion of the mesonet. Elevation angle is 0.5 °. Range rings are every 5 km and locations of mesonet stations and airport runways are overlaid.*

V. SUMMARY

There were 184 microbursts identified which impacted the surface mesonet in Denver between 11 April and 13 September 1988. Both radar and surface data were available for 155 of the events, and 97% of these microbursts were observable by radar. The observability of weak microbursts (less than 20 m/s differential velocity) was actually slightly greater than that of strong microbursts (98% compared to 96%), a result not found in previous studies of microburst observability. One of the two strong microbursts unobservable by radar was the result of low SNR, a cause which shows no obvious correlation to microburst strength. The other strong event was initially unobservable due to asymmetric outflow, and subsequently unobservable due to low SNR. The other two unobservable microbursts were due to 1) asymmetric outflow observed from an unfavorable angle, and 2) shallow outflow below the height of the lowest radar elevation scan.

The 97% microburst observability during 1988 was an increase from 94% in Denver during 1987. Results from a common data collection period during 1987 and 1988 show a similar number of Microburst Days each year, with a significant increase in microburst frequency (and consequently microbursts per Microburst Day frequency) in 1988. It is not known which of the two years represents a more "typical" frequency for Denver, but the comparison implies a wide range of annual variability in microburst frequency that is possible for a given location. Comparison with 1986 results shows a lesser frequency of Microburst Days in Huntsville, AL. Fewer microbursts identified in Huntsville during a common data collection period, in light of the much larger Huntsville mesonet, implies a considerably greater microburst frequency in Denver. Observability by single–Doppler radar in Huntsville was slightly greater (98%), likely due to the absence of any significant SNR problems in the wetter environment.

The diurnal frequency distribution of microbursts shows that more than half of all microbursts identified in 1988 occurred between 2 P.M. and 5 P.M. Local Daylight Time. The monthly distribution shows June and July to be the most active months for microburst occurrence, consistent with results from previous years. A high frequency was also found in April; there was *not* evidence of this in previous years, but the limited data suggests that springtime (April–May) microburst occurrence in general is more common in Denver than in Huntsville.

A comparison of radar and mesonet measurements shows that, on average, the maximum differential velocity measured by radar occurs approximately one minute earlier than that measured by mesonet, while the magnitude of the mesonet measurement is 2 m/s (about 10%) greater. The timing difference provides evidence that sensing aloft may afford more timely wind shear warning information. The difference in estimates of maximum differential velocity perhaps indicates a physical difference in wind shear strength at different heights, but it may also be at least partially the result of the two distinctly different wind sensing systems.

VI. FUTURE WORK

With the deployment of TDWR radars at major U.S. airports, the future disposition of the existing LLWAS sensors is under consideration. Methods are currently being investigated to integrate TDWR and LLWAS in order to provide a unified wind shear warning system that takes advantage of the attributes of each sub-system, while also safeguarding against the deficiencies of each. Continued research involving radar and mesonet data will therefore focus on gaining a better understanding of the relationship between the wind estimates derived from the two sensing methods. In particular, the following questions will be addressed:

(1) What correlation is there between the wind speed and direction provided by a surface sensor and the corresponding radial velocity measured from low-elevation radar scans?

(2) What is the timing relationship between microburst observability by radar and surface sensors? How do the magnitudes of their wind shear estimates compare?

(3) How do wind and divergence estimates of radar and surface sensors compare to pilot reports of wind shear and turbulence?

A clearer understanding of these relationships will be useful in assessing the potential effectiveness and possible drawbacks to proposed TDWR/LLWAS integration schemes.

REFERENCES

Campbell, S. D., 1988: Microburst Precursor Recognition Using an Expert System Approach. Preprints, 4th International Conference on Interactive Information processing Systems for Meteorology, Oceanography, and Hydrology, Anaheim, CA, pp. 300–307.

Campbell, S. D., M. W. Merritt and J.T. DiStefano, 1989: Microburst Recognition Performance of TDWR Operational Testbed. Preprints, 3rd International Conference on the Aviation Weather System, January, 1989, Anaheim, CA.

Campbell, S. D., and M. Merritt, 1987: Advanced Microburst Recognition Algorithm. MIT, Lincoln Laboratory Weather Radar Project Report ATC–145, FAA Report DOT/FAA/PM–87–23.

Clark, D. A., 1988: Observability of Microbursts with Doppler Weather Radar During 1986 in Huntsville,Alabama. MIT, Lincoln Laboratory Project Report ATC–160.

Clark, D. A., and J.T. DiStefano, 1989: Analysis of Microburst Observability with Doppler Radar Through Comparison of Radar and Surface Wind Sensor Data. Preprints, 23rd Conference on Radar Meteorology. Tallahassee, FL, American Meteorological Society, pp. 171–174.

DiStefano, J. T., 1987: Study of Microburst Detection Performance During 1985 in Huntsville, Alabama. MIT, Lincoln Laboratory Project Report ATC–142.

DiStefano, J.T., 1988: Observability of Microbursts Using Doppler Weather Radar and Surface Anemometers During 1987 in Denver, CO. MIT, Lincoln Laboratory Report ATC–161.

Evans, J. E., and D. Turnbull, 1985: The FAA/MIT Lincoln Laboratory Doppler Weather Radar Program. Preprints, 2nd International Conference on the Aviation Weather System. Montreal, Canada, American Meteorological Society, pp. 76–79.

Fujita, T.T., 1980: Downbursts and Microbursts: An Aviation Hazard. Preprints, 11th Conference on Radar Meteorology, Miami Beach, American Meteorological Society, pp. 94–101.

Fujita, T. T., 1985: The Downburst – Microburst and Macroburst. Department of Geophysical Sciences, The University of Chicago, IL, 122 p.

Merritt, M. W., 1987: Automated Detection of Microburst Windshear for Terminal Doppler Weather Radar. Preprints, Digital Image Processing and Visual Communications Technologies in Meteorology. Bellingham, WA, Society of Photo– Optical Instrumentation Engineers (SPIE), pp. 61–68.

National Research Council, 1983: Low Altitude Wind Shear and its Hazard to Aviation. National Academy Press, 112 p.

Wilson, J.W., R.D. Roberts, C. Kessinger, J. McCarthy, 1984: *Microburst Wind Structure and Evaluation of Doppler Radar for Airport Wind Shear Detection.* Journal of Climate and Applied Meteorology, **23**, 895–915.

Wolfson, M. M., J. T. DiStefano, and B. E. Forman, 1987: The FLOWS Automatic Weather Station Network in Operation. MIT, Lincoln Laboratory Project Report ATC-134, FAA Report DOT-FAA-PM-85/27, 284 pp.

Appendix A. Microbursts Impacting the 1988 Denver Mesonet

Explanations: MB# = Microburst Identification Number. Symbols (* or #) next to MB# indicate microbursts which are associated with one or more other microbursts on that day (marked by same symbol) as part of a Divergence Line or Microburst Pulse. Duration refers to time period during which a divergence was detected by the mesonet (not necessarily above microburst threshold). Mesonet Observation: Y=Yes, N=No. FL-2/UND Observation: Y=Yes, N=No, NA= Not Applicable, ND = No Data, I=Incomplete Data. Location is range/azimuth with respect to FL-2. ΔR= Distance between velocity couplet extrema at time of Maximum ΔV. (Although some microbursts show ΔR greater than 4 km, they are nonetheless required to meet the necessary shear threshold of 10 m/s differential velocity over a distance of not greater than 4 km.)Times refer to time of Maximum ΔV as observed by radar and mesonet, respectively

| MB# | Date | Duration (UTC) | Observed By: | | | Location (km,deg) | RADAR | | | | MESONET | |
			Meso	FL-2	UND		Max ΔV (m/s)	Couplet (m/s)	ΔR (km)	Time (UTC)	Max ΔV (m/s)	Time (UTC)
1*	16 Apr	2231–2304	Y	Y	NA	20,315	13	7,–6	5	2256	17	2301
2*	16 Apr	2257–2304	Y	Y	NA	18,330	15	13,–2	3	2301	17	2300
3*	16 Apr	2305–2320	Y	Y	NA	20,325	14	8,–6	3	2311	20	2307
4	19 Apr	1817–1832	Y	Y	NA	16,290	22	7,–15	5	1821	20	1820
5	19 Apr	1819–1828	Y	Y	NA	17,305	18	5,–13	5	1823	15	1827
6*	19 Apr	1822–1830	Y	Y	NA	16,320	14	8,–6	5	1823	16	1825
7*	19 Apr	1828–1842	Y	Y	NA	17,335	14	7,–7	6	1835	22	1834
8	19 Apr	1832–1845	Y	Y	NA	13,285	18	8,–10	5	1837	25	1836
9#	19 Apr	1836–1847	Y	Y	NA	11,315	16	9,–7	4	1839	17	1840
10#	19 Apr	1838–1847	Y	Y	NA	11,295	16	8,–8	4	1841	14	1846
11	21 Apr	0035–0044	Y	Y	NA	18,320	10	4,–6	2	0039	11	0038
12	21 Apr	0040–0047	Y	Y	NA	16,325	13	6,–7	3	0037	16	0044
13*	21 Apr	2117–2132	Y	Y	NA	17,315	25	14,–11	2	2128	32	2128
14*	21 Apr	2128–2202	Y	Y	NA	17,335	25	17,–8	5	2133	38	2135
15	21 Apr	2132–2147	Y	Y	NA	14,305	12	6,–6	3	2135	20	2139
16	21 Apr	2158–2209	Y	Y	NA	13,305	11	5,–6	2	2203	16	2205

Microbursts Impacting the 1988 Denver Mesonet (continued)

| | | | Observed By: | | | | RADAR | | | | MESONET | |
MB#	Date	Duration (UTC)	Meso	FL-2	UND	Location (km,deg)	Max ΔV (m/s)	Couplet (m/s)	ΔR (km)	Time (UTC)	Max ΔV (m/s)	Time (UTC)
17	24 Apr	0103-0120	Y	ND	ND	15,310	--	---	-	--	14	0110
18	24 Apr	0106-0147	Y	ND	ND	12,280	--	---	-	--	19	0131
19	24 Apr	0115-0123	Y	ND	ND	14,325	--	---	-	--	15	0119
20	24 Apr	2001-2021	Y	Y	NA	16,315	13	5,-8	3	2008	21	2012
21	24 Apr	2019-2025	Y	Y	NA	11,320	14	6,-8	3	2016	12	2023
22	24 Apr	2324-2333	Y	ND	ND	21,325	--	---	-	--	11	2327
23	28 Apr	2224-2230	Y	ND	ND	11,290	--	----	-	--	14	2229
24	28 Apr	2231-2249	Y	ND	ND	14,310	--	----	-	--	18	2234
25	28 Apr	2247-2256	Y	ND	ND	18,315	--	----	-	--	19	2249
26	29 Apr	2114-2130	Y	Y	NA	15,305	14	5,-9	2	2123	20	2118
27	29 Apr	2118-2124	Y	Y	NA	13,305	14	3,-11	2	2119	18	2119
28	10 May	1853-1901	Y	Y	NA	17,295	15	7,-8	2	1850	13	1858
29*	10 May	1858-1924	Y	Y	NA	13,320	15	4,-11	3	1908	16	1905
30	10 May	1900-1904	Y	Y	NA	14,300	10	1,-9	2	1856	14	1902
31*	10 May	1902-1925	Y	Y	NA	15,295	14	3,-11	2	1904	14	1906
32	13 May	2044-2053	Y	ND	ND	21,320	--	----	-	--	23	2049
33	13 May	2138-2144	Y	ND	ND	15,300	--	----	-	--	12	2136
34	13 May	2218-2224	Y	Y	NA	15,310	16	10,-6	3	2219	15	2220
35	14 May	2145-2152	Y	I	ND	13,280	--	----	-	--	12	2152
36	17 May	2018-2025	Y	ND	I	16,315	--	----	-	--:	15	2024
37	17 May	2024-2030	Y	ND	Y	17,340	12	4,-8	1	2023	16	2029

A-2

Microbursts Impacting the 1988 Denver Mesonet (continued)

			Observed By:				RADAR				MESONET	
MB#	Date	Duration (UTC)	Meso	FL-2	UND	Location (km,deg)	Max ΔV (m/s)	Couplet (m/s)	ΔR (km)	Time (UTC)	Max ΔV (m/s)	Time (UTC)
38	18 May	0035–0040	Y	ND	ND	14,325	--	---	-	--	22	0037
39	18 May	2138–2158	Y	Y	NA	12,290	21	7,–14	8	2153	16	2158
40	18 May	2142–2149	N	Y	NA	13,325	16	4,–12	4	2147	9	2148
41	18 May	2159–2225	Y	Y	NA	13,330	14	3,–11	3	2211	20	2200
42	21 May	2047–2051	Y	Y	NA	19,330	17	–2,–19	4	2049	19	2049
43	21 May	2054–2058	Y	Y	NA	15,305	15	1,–14	3	2057	21	2057
44	21 May	2100–2106	Y	Y	NA	13,285	16	6,–10	3	2101	15	2103
45	26 May	2035–2041	Y	N	N	16,315	--	---	-	--	14	2036
46	26 May	2037–2043	Y	Y	NA	14,315	10	4,–6	3	2040	12	2039
47	26 May	-----	N	Y	NA	11,315	11	5,–6	2	2046	--	---
48	26 May	2205–2215	Y	Y	NA	13,330	18	10,–8	3	2210	14	2210
49*	26 May	2230–2239	Y	Y	NA	17,320	14	7,–7	3	2234	22	2238
50*	26 May	2240–2245	Y	Y	NA	16,325	13	4,–9	2	2240	13	2242
51	27 May	1842–1900	Y	ND	N	14,295	--	---	-	--	24	1849
52	27 May	2100–2120	Y	N	N	19,325	--	---	-	--	30	2109
53	28 May	0127–0133	Y	ND	ND	18,295	--	---	-	--	20	0130
54	9 June	2050–2059	Y	Y	NA	20,320	20	17,–3	3	2050	23	2054
55*	9 June	2055–2059	Y	Y	NA	17,325	13	11,–2	2	2057	12	2056
56	9 June	2056–2101	Y	Y	NA	14,320	15	11,–4	2	2057	13	2058
57*	9 June	2058–2105	Y	Y	NA	18,315	13	9,–4	3	2101	19	2102
58	9 June	2105–2112	Y	Y	NA	13,285	14	15,1	2	2104	14	2111
59	9 June	2109–2121	Y	Y	NA	20,320	18	12,–6	4	2112	19	2117

A-3

Microbursts Impacting the 1988 Denver Mesonet (continued)

MB#	Date	Duration (UTC)	Observed By:			Location (km,deg)	RADAR				MESONET	
			Meso	FL-2	UND		Max ΔV (m/s)	Couplet (m/s)	ΔR (km)	Time (UTC)	Max ΔV (m/s)	Time (UTC)
60	9 June	2109–2119	Y	Y	NA	11,280	11	11,0	2	2112	14	2116
61	9 June	2123–2131	Y	Y	NA	20,340	17	11,–6	3	2128	24	2125
62	9 June	2144–2157	Y	Y	NA	15,320	18	9,–9	4	2148	17	2154
63	9 June	2203–2234	Y	Y	NA	11,315	19	11,–8	3	2220	16	2220
64	9 June	2232–2245	N	Y	NA	11,285	11	8,–3	3	2232	--	----
65	9 June	2234–2238	N	Y	NA	15,315	12	8,–4	4	2232	9	2238
66	10 June	0137–0148	Y	ND	ND	18,335	--	---	–	--	16	0143
67*	10 June	2144–2159	Y	Y	NA	18,305	38	11,–27	8	2153	29	2148
68*	10 June	2153–2157	Y	Y	NA	19,305	23	11,–12	5	2153	23	2155
69*	10 June	2156–2212	Y	Y	NA	16,315	20	7,–13	3	2158	42	2157
70*	10 June	2200–2205	Y	Y	NA	17,320	13	9,–4	2	2202	21	2202
71	15 June	2222–2244	Y	Y	NA	12,290	17	12,–5	3	2232	14	2231
72	16 June	2210–2220	N	Y	NA	11,290	16	5,–11	3	2216	--	----
73	16 June	2213–2230	Y	Y	NA	18,340	22	9,–13	4	2216	16	2218
74	19 June	0017–0031	Y	ND	ND	18,330	--	---	–	--	14	0018
75	20 June	0353–0401	Y	Y	NA	14,325	13	10,–3	2	0356	16	0355
76	20 June	0356–0412	Y	Y	NA	20,320	11	7,–4	3	0402	24	0405
77	20 June	0410–0416	Y	Y	NA	20,325	14	9,–5	2	0414	18	0411
78	20 June	0415–0420	N	Y	NA	11,285	10	3,–7	1	0418	9	0418
79	20 June	0418–0426	N	Y	NA	17,305	11	6,–5	2	0420	9	0421

Microbursts Impacting the 1988 Denver Mesonet (continued)

MB#	Date	Duration (UTC)	Observed By: Meso	FL-2	UND	Location (km,deg)	RADAR Max ΔV (m/s)	Couplet (m/s)	ΔR (km)	Time (UTC)	MESONET Max ΔV (m/s)	Time (UTC)
80	21 June	1940–1955	Y	Y	NA	20,315	10	6,−4	3	1944	11	1950
81*	21 June	1949–2001	Y	Y	NA	12,305	19	11,−8	5	1958	18	1956
82*	21 June	1952–2010	Y	Y	NA	14,295	21	14,−7	3	2000	31	1956
83	21 June	1959–2004	Y	Y	NA	11,300	25	4,−21	3	2002	25	2004
84	21 June	2002–2011	Y	Y	NA	16,310	10	8,−2	3	2004	12	2004
85	21 June	2003–2007	Y	Y	NA	12,295	14	8,−6	2	2004	13	2006
86#	21 June	2004–2010	Y	Y	NA	10,300	14	6,−8	2	2008	19	2009
87#	21 June	2011–2019	Y	Y	NA	12,285	11	6,−5	2	2015	12	2014
88	21 June	2139–2207	Y	Y	NA	22,315	16	7,−9	7	2148	16	2158
89	22 June	2246–2258	Y	Y	NA	9,315	18	13,−5	4	2254	17	2257
90	22 June	2249–2303	Y	Y	NA	11,325	14	12,−1	2	2302	12	2250
91	25 June	2001–2028	Y	Y	NA	12,320	28	15,−13	3	2012	31	2017
92	25 June	2006–2014	Y	Y	NA	17,340	16	10,−6	3	2006	11	2006
93	25 June	2007–2013	Y	Y	NA	13,280	13	6,−7	2	2012	15	2012
94	25 June	2022–2025	Y	Y	NA	18,305	19	8,−11	2	2022	14	2022
95	26 June	0145–0155	Y	ND	ND	11,290	--	---	-	--	15	0154
96	26 June	0151–0207	Y	ND	ND	14,310	--	---	-	--	20	0202
97	29 June	0015–0030	Y	Y	NA	21,335	14	8,−6	4	0020	11	0025
98	29 June	0019–0030	Y	Y	NA	20,330	11	4,−7	3	0022	11	0020

Microbursts Impacting the 1988 Denver Mesonet (continued)

MB#	Date	Duration (UTC)	Meso	FL-2	UND	Location (km,deg)	RADAR Max ΔV (m/s)	RADAR Couplet (m/s)	RADAR ΔR (km)	RADAR Time (UTC)	MESONET Max ΔV (m/s)	MESONET Time (UTC)
99	2 July	2152–2210	Y	Y	NA	22,320	31	13,–18	6	2154	34	2155
100	2 July	2208–2222	Y	Y	NA	19,305	25	13,–12	10	2211	20	2214
101	2 July	2211–2225	Y	N	Y	18,325	14	6,–8	2	2213	21	2213
102	2 July	2222–2237	Y	Y	NA	17,290	19	6,–13	6	2224	18	2225
103	2 July	2234–2242	Y	Y	NA	13,275	21	13,–8	3	2234	27	2241
104	4 July	2225–2230	N	Y	NA	10,315	12	4,–8	2	2226	7	2227
105	7 July	2344–2355	Y	Y	NA	10,325	16	13,–3	3	2352	23	2245
106	7 July	2356–0019	Y	Y	NA	8,325	17	14,–3	3	0000	19	0002
107	8 July	0013–0023	Y	Y	NA	12,305	11	11,0	2	0014	23	0016
108	8 July	0022–0040	Y	Y	NA	15,295	13	10,–3	2	0025	21	0028
109*	8 July	0024–0045	Y	Y	NA	10,305	23	14,–9	8	0037	24	0030
110*	8 July	0027–0045	Y	Y	NA	8,325	26	15,–11	10	0039	15	0039
111	10 July	0130–0220	Y	Y	NA	9,330	28	14,–14	12	0149	27	0157
112	10 July	0131–0140	Y	Y	NA	16,335	15	11,–4	4	0135	13	0131
113*	10 July	0242–0258	Y	Y	NA	13,315	11	10,–1	3	0241	11	0253
114*	10 July	0256–0313	Y	ND	ND	15,310	--	---	--	---	12	0257
115*	11 July	2206–2212	Y	Y	NA	12,295	18	6,–12	3	2208	24	2212
116*	11 July	2208–2217	Y	Y	NA	8,315	32	16,–16	2	2211	36	2212
117*	11 July	2213–2221	Y	Y	NA	12,300	24	8,–16	2	2215	22	2219
118	11 July	2219–2233	Y	Y	NA	15,295	14	3,–11	3	2230	19	2228
119*	11 July	2222–2227	Y	Y	NA	11,305	27	11,–16	3	2220	24	2222
120*	11 July	2228–2237	Y	Y	NA	11,305	20	10,–10	2	2226	24	2230

Microbursts Impacting the 1988 Denver Mesonet (continued)

			Observed By:				RADAR				MESONET	
MB#	Date	Duration (UTC)	Meso	FL-2	UND	Location (km,deg)	Max ΔV (m/s)	Couplet (m/s)	ΔR (km)	Time (UTC)	Max ΔV (m/s)	Time (UTC)
121	11 July	2230–2233	Y	Y	NA	11,285	16	3,–13	2	2233	21	2231
122	11 July	2233–2250	Y	Y	NA	15,290	13	5,–8	2	2238	20	2236
123	14 July	0416–0426	Y	ND	ND	12,305	--	---	--	----	20	0418
124	14 July	0431–0440	Y	ND	ND	18,320	--	---	--	----	21	0435
125	16 July	2153–2217	Y	Y	NA	20,320	22	6,–16	4	2201	31	2202
126	16 July	2218–2240	Y	Y	NA	19,315	22	7,–15	9	2226	31	2223
127	16 July	2241–2301	Y	Y	NA	16,310	21	8,–13	10	2250	19	2251
128	16 July	2301–2328	Y	Y	NA	14,290	26	13,–13	4	2318	29	2312
129*	16 July	2309–2320	Y	Y	NA	21,325	22	10,–12	2	2310	26	2313
130*	16 July	2316–2328	Y	Y	NA	20,325	20	9,–11	5	2320	23	2325
131	16 July	2320–2331	Y	Y	NA	15,310	13	5,–8	2	2324	17	2324
132	16 July	2323–2338	Y	Y	NA	18,330	18	10,–8	7	2328	23	2327
133	16 July	2329–2346	Y	Y	NA	13,295	20	10,–10	3	2334	20	2330
134#	16 July	2342–2359	Y	Y	NA	8,300	31	18,–13	13	2348	25	2347
135#	16 July	2351–2359	Y	Y	NA	15,320	17	13,–4	6	2354	19	2357
136	17 July	0014–0019	Y	Y	NA	13,325	13	5,–8	3	0010	23	0017
137	17 July	0013–0022	Y	Y	NA	18,325	12	8,–4	3	0016	13	0016
138	17 July	0023–0027	Y	Y	NA	10,325	11	3,–8	2	0020	16	0025
139	17 July	0024–0034	Y	N	Y	20,330	16	10,–6	3	0027	14	0033
140	17 July	---	N	Y	NA	13,325	18	6,–12	2	0030	--	---
141	17 July	0035–0049	Y	Y	NA	13,315	19	14,–5	2	0044	23	0043
142*	17 July	2134–2151	Y	Y	NA	15,300	22	8,–14	8	2144	26	2140
143*	17 July	2141–2157	Y	Y	NA	11,280	22	11,–11	5	2150	27	2142

Microbursts Impacting the 1988 Denver Mesonet (continued)

							RADAR				MESONET	
MB#	Date	Duration (UTC)	Meso	FL-2	UND	Location (km,deg)	Max ΔV (m/s)	Couplet (m/s)	ΔR (km)	Time (UTC)	Max ΔV (m/s)	Time (UTC)
144	23 July	2143-2149	Y	Y	NA	11,280	13	-9,-22	3	2145	20	2146
145	23 July	2152-2201	Y	Y	NA	14,325	16	-6,-22	4	2157	20	2155
146	23 July	2202-2209	Y	Y	NA	23,320	23	6,-17	3	2159	22	2203
147	29 July	2253-2307	Y	Y	NA	17,310	11	14,3	3	2257	17	2300
148	2 Aug	0252-0257	Y	ND	ND	15,310	---	----	--	----	27	0255
149	2 Aug	0258-0308	Y	ND	ND	15,315	--	---	--	---	27	0300
150*	8 Aug	2023-2031	Y	Y	NA	13,280	16	1,-15	2	2026	15	2028
151*	8 Aug	2033-2043	Y	Y	NA	12,275	17	5,-12	2	2030	19	2038
152	9 Aug	1849-1900	Y	Y	NA	17,305	24	10,-14	3	1848	27	1850
153*	9 Aug	1857-1904	Y	Y	NA	18,305	21	8,-13	3	1902	31	1859
154*	9 Aug	1900-1910	Y	Y	NA	17,310	25	11,-14	3	1902	26	1908
155*	9 Aug	1902-1907	Y	Y	NA	17,320	26	13,-13	3	1904	34	1904
156*	9 Aug	1905-1914	Y	Y	NA	17,320	22	9,-13	2	1908	35	1908
157	9 Aug	1914-1917	Y	Y	NA	15,325	12	6,-6	1	1912	17	1914
158	9 Aug	1916-1922	Y	Y	NA	18,310	21	8,-13	2	1916	26	1921
159	9 Aug	1923-1929	Y	Y	NA	17,325	22	11,-11	2	1922	23	1927
160#	9 Aug	1923-1930	Y	Y	NA	17,305	20	11,-9	3	1932	30	1925
161#	9 Aug	1927-1936	Y	Y	NA	17,295	15	9,-16	3	1928	17	1931
162#	9 Aug	1928-1930	Y	Y	NA	17,335	14	6,-8	2	1928	14	1928
163#	9 Aug	1931-1957	Y	Y	NA	14,330	28	14,-14	3	1938	25	1936
164	9 Aug	1937-1945	Y	Y	NA	17,305	11	3,-8	3	1938	10	1937
165	9 Aug	1949-2002	Y	Y	NA	9,290	23	9,-14	4	1958	19	1952

A-8

Microbursts Impacting the 1988 Denver Mesonet (continued)

MB#	Date	Duration (UTC)	Observed By: Meso	FL-2	UND	Location (km,deg)	RADAR Max ΔV (m/s)	Couplet (m/s)	ΔR (km)	Time (UTC)	MESONET Max ΔV (m/s)	Time (UTC)
166	12 Aug	2159–2206	Y	Y	NA	14,290	21	7,–14	5	2204	16	2203
167	12 Aug	2205–2211	Y	Y	NA	14,280	22	7,–15	5	2205	19	2210
168	12 Aug	2207–2214	Y	Y	NA	12,305	18	5,–13	4	2207	14	2213
169	12 Aug	2207–2219	Y	Y	NA	13,320	17	6,–11	3	2207	19	2213
170	20 Aug	2034–2045	Y	Y	NA	16,290	19	11,–8	5	2039	17	2040
171	20 Aug	2039–2042	Y	Y	NA	13,275	18	1,–17	2	2037	13	2041
172	26 Aug	---	N	Y	NA	13,320	12	4,–8	2	2302	--	---
173	27 Aug	0202–0212	Y	ND	ND	16,310	--	---	--	---	15	0210
174	27 Aug	0203–0209	Y	ND	ND	17,320	--	---	--	---	18	0206
175	27 Aug	0205–0217	Y	ND	ND	16,315	--	---	--	---	19	0206
176	27 Aug	0214–0221	Y	ND	ND	17,330	--	---	--	---	13	0219
177	27 Aug	0223–0233	Y	ND	ND	17,305	--	---	--	---	11	0228
178	10 Sep	2119–2127	Y	Y**	NA	10,305	(14)	(4,–10)	(3)	(2125)	14	2120
179	10 Sep	2240–2259	Y	Y	NA	14,310	16	6,–10	4	2249	16	2250
180	10 Sep	2246–2249	Y	Y	NA	14,280	17	4,–13	5	2242	14	2246
181	10 Sep	2302–2307	Y	Y	NA	13,300	11	6,–5	2	2304	15	2305
182	10 Sep	2321–2323	Y	Y	NA	12,330	17	14,–3	7	2322	15	2323
183	10 Sep	2317–2333	Y	Y	NA	20,310	17	10,–7	5	2322	18	2327
184	10 Sep	2325–2333	Y	Y	NA	19,325	14	13,–1	2	2327	12	2328

** Radar data for MB #178 was incomplete, although the microburst signature was identifiable.